

Partially Coherent Waves in Nonlinear Periodic Lattices

*By H. Buljan, G. Bartal, O. Cohen, T. Schwartz, O. Manela, T. Carmon,
M. Segev, J. W. Fleischer, and D. N. Christodoulides*

We study the propagation of partially coherent (random-phase) waves in nonlinear periodic lattices. The dynamics in these systems is governed by the threefold interplay between the nonlinearity, the lattice properties, and the statistical (coherence) properties of the waves. Such dynamic interplay is reflected in the characteristic properties of nonlinear wave phenomena (e.g., solitons) in these systems. While the propagation of partially coherent waves in nonlinear periodic systems is a universal problem, we analyze it in the context of nonlinear photonic lattices, where recent experiments have proven their existence.

1. Introduction

Nonlinear periodic systems are frequently encountered in nature. Examples may be found in biology [1], solid-state physics [2], nonlinear optics [3], Josephson ladders [4], Bose–Einstein condensates (BEC) [5], etc. The behavior of waves in periodic systems is driven by the interference (e.g., interference is responsible for the existence of bands and band gaps in the spectra of the linear periodic systems [6, 7]), which crucially depends on the coherence of waves. This fact implies that waves with only partial coherence can exhibit

Address for correspondence: M. Segev, Physics Department, Technion, Israel Institute of Technology, Haifa 32000, Israel; e-mail: msegev@techunix.technion.ac.il

different features than fully coherent waves in nonlinear periodic systems. However, in spite of the considerable attention that was given to the problem of wave propagation in nonlinear periodic lattices [3, 8–49], the propagation of partially coherent waves (PCWs) in such systems has not been studied until recently [37, 45, 46]. This direction of research is further motivated by the fact that most waves encountered in nature are only partially coherent. Partial coherence of waves becomes important when fluctuations (thermal, quantum, or other) reduce the correlation distances to magnitudes comparable with the characteristic length scales of the periodic system, e.g., the lattice spacing. In this case, the dynamics is governed by the threefold interplay between the statistical (coherence) properties of the waves, the lattice periodicity, and the nonlinearity. The consequences of this interplay are observed in the characteristic features of partially coherent solitons in nonlinear periodic lattices [37, 45].

Here we present a comprehensive theoretical [37] and experimental [45] study of partially coherent lattice solitons, also called random-phase lattice solitons (RPLSs). These solitons exist when linear transport (diffraction) in the lattice is balanced by nonlinear self-focusing (or defocusing) effects. The properties of such solitons, namely, their intensity structure, statistical (coherence) properties, and spatial power spectra, all conform to the lattice periodicity [37, 45]. Perhaps the most interesting feature of the RPLSs is found in the momentum space (\mathbf{k} -space), which is partitioned into Brillouin zones (BZ) due to the periodicity of the system [6, 7]. The Floquet–Bloch power spectrum of RPLSs is multihumped with humps being located in the normal (anomalous) diffraction regions of the BZs in the case of a self-focusing (defocusing, respectively) nonlinearity. The experiment of [45] has shown that an incoherent wavepacket with a simple bell-shaped intensity structure and a bell-shaped Fourier power spectrum may, under proper nonlinear conditions, evolve into a self-trapped beam with the characteristic RPLS properties. The physical mechanism underlying this observation is the fact that, under proper conditions, nonlinearity transfers the energy between the modes of the linear system in a specific fashion that leads to RPLS formation. We present here a theoretical study of this type of dynamics, illustrating the evolution of the intensity structure and the power spectrum of an incoherent beam into a RPLS, in both one and two transverse dimensional geometry.

The dynamics of PCWs in nonlinear periodic lattices is relevant to various fields of research. In this paper, we focus on nonlinear optical systems, and study the propagation of partially spatially coherent waves in nonlinear waveguide arrays. One of the key physical mechanisms in our system is the noninstantaneous response of the nonlinearity: the nonlinearity cannot follow fast fluctuations of the field, but rather responds to the time-averaged intensity. This optical system is analogous to incoherent matter waves (matter waves

involving a Bose–Einstein condensate and particles in excited states) in optical lattices.

Our current studies of PCWs in nonlinear periodic lattices draw upon two directions of research that have received considerable attention in recent years: (1) partially coherent light waves in homogeneous nonlinear media [50–77], and (2) coherent light waves in nonlinear periodic lattices [3, 8–49]. For this reason, Section 2 provides a brief outline of the results from these two directions of research that are most relevant to our current studies. The rest of the paper is organized as follows. Section 3 describes the physical system considered in [37, 45, 46], and the theoretical model(s) used for its description. Section 4 discusses the dynamics of partially coherent waves in linear periodic lattices. In Section 5 we focus on the theoretical description of RPLSs [37], while in Section 6 we review some facts from the experimental observation of RPLSs [45]. Section 7 presents a theoretical study of the dynamical evolution of an incoherent beam with a simple bell-shaped intensity structure and power spectrum into an incoherent beam with the complex RPLS characteristics. In Section 8 we conclude.

2. Background

The behavior of partially coherent light in nonlinear photonic lattices has been recently studied in the context of RPLSs, both theoretically [37] and experimentally [45], and in the context of developing a novel experimental technique for Brillouin zone spectroscopy (BZS) of linear and nonlinear photonic lattices [46]. All previous studies of nonlinear phenomena (e.g., solitons and modulation instability (MI)) with partially coherent light were performed in homogeneous nonlinear media [50–77]. On the other hand, the propagation of light in nonlinear periodic lattices was previously studied only with coherent waves [3, 8–49]. In our current pursuit for the understanding of PCWs in nonlinear photonic lattices we draw upon two directions of research: (1) partially coherent light waves in homogeneous isotropic nonlinear media, and (2) coherent light waves in nonlinear periodic lattices. Below, we briefly outline some of the results from these two directions of research that are most relevant to our current studies.

2.1. Partially coherent light waves in homogeneous nonlinear media

The nonlinear dynamics of partially coherent light in homogeneous nonlinear media has been extensively studied since the first observation of spatially incoherent solitons [50], and incoherent white-light solitons [51]. The light source used in [50] was a laser beam sent through a rotating diffuser, which

generated spatially incoherent, quasimonochromatic, light beam, equivalent to light emitted by a quasithermal source [78, 79]. The incoherent white-light soliton experiment [51] used an ordinary incandescent light bulb generating light with a temporal spectrum that spans the entire visible range; in that experiment the light was both spatially and temporally incoherent. The diffraction of such an incoherent beam depends not only on the size of the beam, but also on its coherence properties; a beam that is more incoherent has a stronger tendency to diffract. When a stable balance between the incoherent beam diffraction and the nonlinearity is achieved, an incoherent soliton is formed. An important physical mechanism employed in [50, 51] for achieving this balance is the noninstantaneous response of the nonlinearity: the nonlinearity is unable to follow fast random fluctuations of the electric field, but rather responds to the time-averaged intensity [50, 51]. This enables the formation of a smooth self-induced waveguide whose modes are randomly populated. The average population of these modes is such that the self-consistency loop is closed [53, 67], which is another way of stating the balance between incoherent beam diffraction and the nonlinearity.

The experiments [50, 51] were followed by a flurry of theoretical and experimental work on partially coherent light in homogeneous nonlinear media. Some of the experimental results include the demonstration of self-trapping of dark incoherent light beams [54], the observation of soliton clustering in weakly correlated wavefronts [68], and the very recent observation of elliptic incoherent solitons [72]. While most of the experiments were thus far performed in photorefractive crystals employing the screening nonlinearity, incoherent spatial solitary waves were also observed in nematic liquid crystals [66]. Besides solitons, the nonlinear phenomenon of MI and spontaneous pattern formation with spatially incoherent light has also been observed with spatially incoherent light, also in noninstantaneous nonlinear medium [62]. The experiment of [62] has demonstrated that MI occurs only when the nonlinearity overcomes a threshold set by the degree of coherence of waves. For light that is less coherent the threshold is higher. This finding has led to the experimental elimination of the transverse instabilities of Kerr solitons [63], and to the observation of “anti-dark” solitons: bright solitons on a background of a uniform beam [61]. In the latter experiment [61], the uniform-component beam was sufficiently spatially incoherent to eliminate MI, whereas the soliton component was fully coherent. In a similar vein, we note a recent observation of stable propagation of spatially localized optical vortices in self-focusing nonlinear medium; the azimuthal instability was arrested by means of spatial incoherence [73]. Another related experiment demonstrated induced MI of incoherent light [65]. Most recently, the phenomenon of MI and spontaneous pattern formation was observed with incoherent white light [76], where an incandescent light bulb has been utilized as the light source. The experiment has shown that all temporal frequencies in the incoherent white-light beam behave

in a collective fashion; they undergo instability at the same threshold value and self-adjust their contributions in the spontaneously formed pattern [76].

On the theoretical side, several different theoretical approaches have been developed for the analysis of incoherent light propagation in noninstantaneous nonlinear media, and various nonlinear phenomena were predicted and explained. There are three formally equivalent theoretical approaches [64], the coherence density theory [52], the modal theory [53], and the mutual coherence function theory [57]. In some cases, one approach may be more suitable than the other to analyze the dynamics, e.g., modal theory seems to be most suitable for the analytical or numerical calculation of spatially incoherent solitons, while the mutual coherence function approach seems to be more suitable for the analysis of MI with incoherent light. In addition to these approaches, an intuitive geometrical optics approach useful for the description of big incoherent solitons was suggested as well [55]. A statistical physics approach based on the Wigner transform was developed and used to analyze incoherent solitons and MI [69]. For the description of the propagation of incoherent white light (both spatially and temporally incoherent light) in noninstantaneous nonlinear media, a model based on the mutual spectral density [70], and other equivalent models [71], were used. The aforementioned theoretical approaches were used for the description of nonlinear phenomena with incoherent light such as bright spatially incoherent solitons [52, 53, 55, 57], dark incoherent solitons [56], and incoherent white light solitons [71]. It was evident from the theoretical papers that incoherent solitons exist and are stable in a broad range of parameters [53]. Incoherent solitons of variable shape were also shown to exist [58], having no coherent equivalent in homogeneous isotropic nonlinear media. The predictions of MI with spatially incoherent light [60], and with incoherent white light [70], were later experimentally confirmed. Regarding the stability of steady-state solutions, although incoherence may eliminate the instability during MI [60], and eliminate the transverse instability of Kerr solitons [63], it has been demonstrated that partially coherent (2+1)D beams in Kerr media undergo catastrophic collapse [59]. Recently, studies of incoherent solitons in instantaneous response nonlinear media [74, 77], and nonlocal incoherent solitons [75] have appeared. Quite generally, all these papers have pointed out that the statistical (coherence) properties of the light greatly influence the features of nonlinear phenomena. For a comprehensive review on partially coherent light in homogeneous noninstantaneous nonlinear media (with emphasis on solitons and MI), see [67].

2.2. Coherent light waves in nonlinear periodic lattices

The dynamics of coherent light waves in nonlinear waveguide arrays has received considerable attention in recent years. Of particular interest is the physics of nonlinear localized modes, such as discrete solitons [29] or breathers

[11, 18, 48]. Solitons in nonlinear waveguide arrays occur when a stable balance is achieved between diffraction of a localized wavepacket in a periodic medium, and the counteracting nonlinear effect. The diffraction of a localized wavepacket in a periodic medium can be both normal and anomalous (see Section 4). The curvature of the phase front during normal diffraction is convex and evolves in the same fashion as in linear homogeneous media (hence the word normal). On the other hand, the curvature evolves in the opposite (concave) fashion during anomalous diffraction. These facts make a great distinction between light propagation in periodic versus homogeneous (uniform) media. As an example, in nonlinear waveguide arrays, bright solitons can form as a balance between nonlinear self-focusing and normal diffraction, or between self-defocusing and anomalous diffraction; the latter case has no counterpart in homogeneous media.

Coherent optical solitons in nonlinear waveguide arrays were predicted in 1988 [3], and observed 10 years later [12]. A number of experiments related to the propagation of coherent wavepackets in linear and nonlinear periodic lattices followed, to name a few: the observations of Bloch oscillations [15, 16], diffraction management [19, 23], spatial gap (staggered) solitons [26, 27], higher band Floquet–Bloch solitons [28], and modulational instability [36]. Coherent lattice solitons were also observed with quadratic nonlinearities [44], and with liquid crystal waveguide arrays [38]. The demonstration of lattice solitons in the (2+1)D geometry [27] opened up the possibility for studying lattice solitons carrying angular momentum, such as vortex lattice solitons [34, 35]. The (2+1)D photonic lattice from [27] was obtained with the use of the optical induction technique proposed in [24]. The same system facilitated the demonstration of 2D dipole-type lattice [41] solitons and 2D vector lattice solitons [42]. This is the system we used for the experimental observation of random-phase lattice solitons [45], and for developing a novel experimental technique for BZS [46]. We note that the optical induction technique for generating 2D nonlinear photonic lattices works not only with interfering plane waves, but also with arrays of incoherent tightly focused beams [17, 43]. However, in that case, if the waves inducing the lattice propagate linearly, their intensity structure necessarily evolves during propagation. The alternative is to have the lattice-inducing waves propagate nonlinearly, in which case they form an array of incoherent solitons [17]; such nonlinear lattices require larger lattice spacings to eliminate the possible instabilities.

Theoretically, nonlinear phenomena in nonlinear waveguide arrays have at first been analyzed by using the discrete nonlinear schrodinger equations (DNLS) [3]. Discrete models were used to describe various nonlinear phenomena in nonlinear periodic systems, e.g., MI [3], self-localization in arrays of defocusing waveguide arrays [8], dark solitons in discrete lattices [9], discrete strongly localized vectorial modes [13], discrete solitons in quadratic nonlinear media [14], soliton interactions and beam steering in nonlinear waveguide arrays [10],

discrete vortex solitons [20], discrete diffraction-managed solitons [22, 25], discrete cavity solitons [40], etc. While discrete models are successful for describing many phenomena, they are not suitable for the analysis of those nonlinear lattice phenomena that involve the excitation of modes from higher bands. The evolution of waves exciting higher bands can be studied through a continuous nonlinear evolution equation with a periodic potential term, utilizing the Floquet–Bloch theory [21, 24]. Because excitation involving incoherent light are broad in \mathbf{k} -space, the latter continuous theoretical model is ubiquitous [37]. Such continuous models have been used for the prediction of solitons in nonlinear optically induced lattices [24], the prediction of multiband vector lattice solitons [30, 31], the theoretical and experimental analysis of nonlinear Bloch-wave interaction and Bragg scattering in optically induced lattices [33], the theoretical study of vortex solitons from the 1st and 2nd bands [34, 39], and the theoretical prediction of random-phase lattice solitons [37].

Several reviews on these nonlinear phenomena were written in recent years, with emphasis on localization of light in nonlinear waveguide arrays [29] and waves in nonlinear photonic crystals [47]. The physics and applications of nonlinear localized modes in various fields is also reviewed in [48, 49].

3. Description of incoherent light in a linear/nonlinear waveguide array

In this section, we describe the physical system under consideration, and the model used for its description. A source of light is partially spatially incoherent and quasimonochromatic. For example, it can be obtained by passing a laser beam through a rotating diffuser [50]. The electric field $E(\mathbf{r}, z, t)$ of the incoherent light is linearly polarized; here $\mathbf{r} = x\mathbf{i} + y\mathbf{j}$ denotes spatial (transverse) coordinates, z is the propagation direction, and t denotes time. The characteristic time of random fluctuations of the electric field, i.e., the coherence time, is denoted with τ_c . The second-order coherence properties of the light are contained within the mutual coherence function [78],

$$B(\mathbf{r}_1, \mathbf{r}_2, z) = \langle E(\mathbf{r}_1, z, t)E^*(\mathbf{r}_2, z, t) \rangle, \quad (1)$$

where brackets $\langle \dots \rangle$ denote the ensemble average, which is equal to the time-average for ergodic sources [78], as is assumed to be the case here. We are interested in the evolution of mutual coherence $B(\mathbf{r}_1, \mathbf{r}_2, z)$ along the propagation axis z .

This partially spatially incoherent continuous wave beam is incident upon a noninstantaneous nonlinear medium (e.g., photorefractives [50], liquid crystals [66]) with a periodically modulated index of refraction. The response time of the nonlinearity τ_m is much longer than the coherence time, $\tau_m \gg \tau_c$; thus the nonlinearity is unable to follow the fast random fluctuations of the field. From this it follows that the nonlinear index change δn is in temporal steady state,

$\partial \delta n / \partial t = 0$; δn depends on the time-averaged intensity $I(\mathbf{r}, z) = B(\mathbf{r}, \mathbf{r}, z)$. The square of the total index of refraction can be written as $n_0^2 + 2n_0 V(\mathbf{r}, z)$, where n_0 denotes the (homogeneous) linear part of the refractive index, while the potential

$$V(\mathbf{r}, z) = p(\mathbf{r}) + \delta n(I(\mathbf{r}, z)) \quad (2)$$

contains both the nonlinear term $\delta n(I(\mathbf{r}, z))$, and the periodic term $p(\mathbf{r})$, which describes the lattice and its properties. In (1 + 1)D problems, $p(x) = p(x + D)$, where D is the lattice spacing. In (2 + 1)D problems, the periodic term is invariant under translations by $\mathbf{R} = n_1 \mathbf{a}_1 + n_2 \mathbf{a}_2$, that is, $p(\mathbf{r}) = p(\mathbf{r} + \mathbf{R})$, where \mathbf{a}_1 and \mathbf{a}_2 are primitive vectors of the lattice and n_1 and n_2 are integers. Note that the periodic term does not vary with the propagation coordinate z . This geometry of the system is referred to as a nonlinear waveguide array [29].

We still need a nonlinear evolution equation to describe the dynamics. By using the paraxial approximation, it can be shown that the randomly fluctuating field obeys [53, 57]

$$i \frac{\partial E}{\partial z} + \frac{1}{2\kappa} \nabla^2 E + \frac{V(\mathbf{r}, z)\kappa}{n_0} E = 0, \quad (3)$$

where $\kappa = n_0 \omega / c$ denotes the wavenumber. From Equation (3) we obtain an equation of motion describing the dynamics of the intensity and statistical properties of the light along the propagation axis:

$$i \frac{\partial B}{\partial z} + \frac{1}{2\kappa} (\nabla_1^2 - \nabla_2^2) B + \frac{\kappa}{n_0} [V(\mathbf{r}_1, z) - V(\mathbf{r}_2, z)] B = 0. \quad (4)$$

The mutual coherence function $B(\mathbf{r}_1, \mathbf{r}_2, z)$ provides the statistical properties of the incoherent light. However, for the analysis of random-phase lattice solitons in terms of the Floquet–Bloch theory [6], it is more fruitful to use the modal theory [53, 64]. Within the modal theory, the electric field is presented as a superposition of coherent waves with randomly varying coefficients $E(\mathbf{r}, z, t) = \sum_m c_m(t) \psi_m(\mathbf{r}, z)$ [53], while the statistics follows from $\langle c_m(t) c_{m'}^*(t) \rangle = d_m \delta_{mm'}$, that is,

$$B(\mathbf{r}_1, \mathbf{r}_2, z) = \sum_m d_m \psi_m(\mathbf{r}_1, z) \psi_m^*(\mathbf{r}_2, z), \quad (5)$$

while $I(\mathbf{r}, z) = \sum_m d_m |\psi_m(\mathbf{r}, z)|^2$. The functions $\psi_m(\mathbf{r}, z)$ form an orthonormal set, and d_m denotes the power within the m th coherent wave [64]. The evolution of coherent waves ψ_m , and consequently of statistical properties (Equation (5)), is governed by a set of equations:

$$i \frac{\partial \psi_m}{\partial z} + \frac{1}{2\kappa} \nabla^2 \psi_m + \frac{V(\mathbf{r}, z)\kappa}{n_0} \psi_m(\mathbf{r}, z) = 0. \quad (6)$$

The mutual coherence function approach [57, 64] is fully equivalent to the modal approach [53, 64].

Equations (4) and/or (6) describe the propagation of spatially incoherent light in noninstantaneous nonlinear media with periodically modulated index of refraction. When the media is linear, i.e., when $V(\mathbf{r}, z) = p(\mathbf{r}, z)$, we can apply the superposition principle, and describe the dynamics by projecting the initial excitation onto the modes of the linear system, the Floquet–Bloch waves, which is described in the next section.

4. Linear dynamics

In the linear case, the dynamics of incoherent light is described by a set of uncoupled evolution equations for the set of wavefunctions $\psi_m(\mathbf{r}, z)$ as

$$i \frac{\partial \psi_m}{\partial z} + \frac{1}{2\kappa} \nabla^2 \psi_m + \frac{p(\mathbf{r})\kappa}{n_0} \psi_m(\mathbf{r}, z) = 0. \quad (7)$$

Each coherent wave $\psi_m(\mathbf{r}, z)$ evolves independently from all other coherent waves. The overall evolution of the statistical properties of the incoherent light, and of the time-averaged intensity, may be obtained from Equation (5).

The evolution of a single coherent wave $\psi_m(\mathbf{r}, z)$ can be traced by projecting it onto the eigenstates of the linear lattice,¹ the Floquet–Bloch (FB) waves $\phi_{n\mathbf{k}}(\mathbf{r}, z) = f_{n\mathbf{k}}(\mathbf{r}) \exp[i\mathbf{k} \cdot \mathbf{r} + i\beta z]$, which are obtained from the spectral equation

$$\frac{1}{2\kappa} \nabla^2 [f_{n\mathbf{k}}(\mathbf{r}) e^{i\mathbf{k} \cdot \mathbf{r}}] + \frac{p(\mathbf{r})\kappa}{n_0} f_{n\mathbf{k}}(\mathbf{r}) e^{i\mathbf{k} \cdot \mathbf{r}} = \beta f_{n\mathbf{k}}(\mathbf{r}) e^{i\mathbf{k} \cdot \mathbf{r}}, \quad (8)$$

where $f_{n\mathbf{k}}(\mathbf{r})$ is a function with the periodicity of the lattice, $f_{n\mathbf{k}}(\mathbf{r}) = f_{n\mathbf{k}}(\mathbf{r} + \mathbf{R})$. Equation (8) is well known from solid-state physics, as it describes the eigenstates of an electron in a periodic potential of an atomic lattice [6]. The index n in the notation for FB waves denotes the band number, while \mathbf{k} is the Bloch wave vector [6, 7]. The Bloch wave vectors are organized into Brillouin Zones (BZs), which are most conveniently illustrated in the extended BZ scheme [6]. The transmission spectrum (a set of real β s) of the FB modes is organized into bands, separated by gaps. The spectral values β depend on the band number n and Bloch wave vector \mathbf{k} , $\beta \equiv \beta(n, \mathbf{k})$ (for brevity, in what follows we do not explicitly write this dependence). For 1D lattices, bands are separated by gaps, whereas for 2D lattices, gaps do not always occur [32]. In spatial optics of waveguide arrays, the spectral values (β s) are the

¹The coherent waves ψ_m are generally not the eigenmodes of the lattice. They depend on the coherence properties of the light contained in the mutual coherence function $B(\mathbf{r}_1, \mathbf{r}_2, z)$, and they can be calculated from an integral eigenvalue equation, $\int B(\mathbf{r}_1, \mathbf{r}_2, z) \psi_m(\mathbf{r}_2, z) d\mathbf{r}_2 = d_m \psi_m(\mathbf{r}_1, z)$, under quite general conditions [78]; d_m are eigenvalues while ψ_m are eigenmodes of the integral equation above.

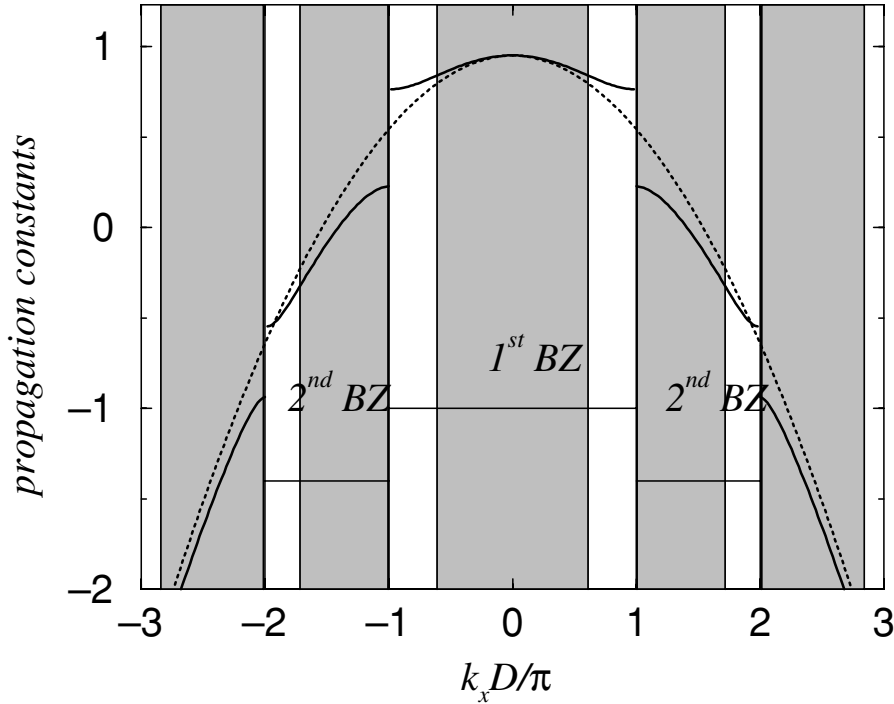


Figure 1. The diffraction curve of a one-dimensional linear periodic lattice (solid lines), and a diffraction curve corresponding to a linear homogeneous isotropic medium (dotted parabola). The propagation constants of the lattice diffraction curve (ordinate) are organized into bands separated by gaps; the first three bands are shown. The k_x -space (abscissa) is partitioned into Brillouin zones; the picture is drawn in the extended zone scheme [6]. The dotted parabola has a negative curvature ($\partial^2 \beta / \partial k_x^2 < 0$) across k_x -space which corresponds to normal diffraction. The periodic system has regions of normal diffraction ($\partial^2 \beta / \partial k_x^2 < 0$, shaded regions), and regions of anomalous diffraction ($\partial^2 \beta / \partial k_x^2 > 0$, white).

propagation constants of the FB propagating modes. In solid-state physics, β corresponds to energy (note that the ordering of propagation constants is up-side-down in comparison with the ordering of energy values).

Consider an example of a spectrum corresponding to a linear 1D photonic lattice with parameters $p(x) = p_0 \sum_m e^{-[(x-mD)/x_0]^8}$, $p_0/n_0 \approx 1.74 \cdot 10^{-4}$, $x_0/D = 0.37$. Figure 1 shows the values of the propagation constants (β) as a function of a Bloch-wave vector (k_x), exemplifying the organization into bands and gaps in the extended BZ scheme. In 1D periodic media, the n th BZ ($n=1, 2, \dots$) is a union of intervals $\pm[(n-1)\pi/D, n\pi/D]$. For comparison, the dotted parabola in Figure 1 denotes the diffraction curve for the homogeneous (and isotropic) linear media.

When an incoherent beam enters a linear waveguide array, at the input face of the medium ($z=0$) each coherent wave $\psi_m(\mathbf{r}, z=0)$ excites a number of

FB waves, which may be written as $\psi_m(\mathbf{r}, z=0) = \sum_{n\mathbf{k}} c_{n\mathbf{k}}^m \phi_{n\mathbf{k}}(\mathbf{r}, z=0)$. The coefficients in the expansion $c_{n\mathbf{k}}^m$ follow from

$$c_{n\mathbf{k}}^m = \int \psi_m(\mathbf{r}, z=0) f_{n\mathbf{k}}^*(\mathbf{r}) e^{-i\mathbf{k}\cdot\mathbf{r}} d\mathbf{r}. \quad (9)$$

Because the system is linear, there is no transfer of energy among the modes of the linear system, and the evolution of $\psi_m(\mathbf{r}, z)$ is simply given by

$$\psi_m(\mathbf{r}, z) = \sum_{n\mathbf{k}} c_{n\mathbf{k}}^m \phi_{n\mathbf{k}}(\mathbf{r}, z) = \sum_{n\mathbf{k}} c_{n\mathbf{k}}^m f_{n\mathbf{k}}(\mathbf{r}) e^{i\mathbf{k}\cdot\mathbf{r}} e^{i\beta z}. \quad (10)$$

The dynamics of each coherent wave is not coupled to the dynamics of the others, hence we may formally write the mutual spectral density,

$$\begin{aligned} B(\mathbf{r}_1, \mathbf{r}_2, z) &= \sum_m \sum_{n\mathbf{k}} \sum_{n'\mathbf{k}'} d_m c_{n\mathbf{k}}^m c_{n'\mathbf{k}'}^{m*} \phi_{n\mathbf{k}}(\mathbf{r}_1, z) \phi_{n'\mathbf{k}'}^*(\mathbf{r}_2, z) \\ &= \sum_m \sum_{n\mathbf{k}} \sum_{n'\mathbf{k}'} d_m c_{n\mathbf{k}}^m c_{n'\mathbf{k}'}^{m*} f_{n\mathbf{k}}(\mathbf{r}_1) f_{n'\mathbf{k}'}^*(\mathbf{r}_2) e^{i\mathbf{k}\cdot\mathbf{r}_1 - i\mathbf{k}'\cdot\mathbf{r}_2} e^{i(\beta - \beta')z}. \end{aligned} \quad (11)$$

The linear dynamics is conceptually simple: at $z=0$ we simply project the initial excitation onto the eigenmodes of the linear system $\phi_{n\mathbf{k}}$, i.e., we calculate the complex coefficients $c_{n\mathbf{k}}^m$ via Equation (9), and trace the evolution of the coherent waves $\psi_m(\mathbf{r}, z)$ and the mutual coherence $B(\mathbf{r}_1, \mathbf{r}_2, z)$ by using Equations (10) and (11), respectively. However, in spite of this conceptual simplicity, even linear dynamics in these systems can possess interesting nontrivial features.

The dynamics of a localized beam entering a linear waveguide array is referred to as diffraction in periodic media, or discrete diffraction. Consider a localized wavepacket exciting the FB waves around some transverse momentum value \mathbf{k} . The diffraction of such wavepacket depends on the curvature of the diffraction manifold at \mathbf{k} . In 1D periodic media, the diffraction coefficient $D_p(k_x) = \partial^2 \beta(k_x) / \partial k_x^2$ oscillates around zero, and the regions of normal [$D_p(k_x) < 0$] and anomalous diffraction [$D_p(k_x) > 0$] alternate (Figure 1). The n th BZ ($n=1, 2, \dots$) is divided into the normal $\pm [(n-1)\pi/D, \alpha_n]$, and anomalous diffraction intervals $\pm (\alpha_n, n\pi/D]$, where $D_p(\alpha_n) = 0$ (Figure 1). Normal diffraction intervals are those where the diffraction curve has the same curvature as the parabola corresponding to free-space diffraction (Figure 1). Thus, the main difference between diffraction in homogeneous media and diffraction in periodic media, is that in the latter case diffraction can be both normal and anomalous. This feature has initiated several studies related to the possibility of diffraction management [19, 22, 23, 25].

The properties of the linear system greatly affect the features of nonlinear wave phenomena in the associated nonlinear system. This is clearly seen in the analysis of the solitary waves (lattice solitons or discrete solitons), which

propagate in the lattice without changing their intensity profile, as discussed in the next section.

5. Random phase lattice solitons: Theory

A localized incoherent wavepacket that enters a linear waveguide array diffracts, that is, it experiences nonstationary propagation (Section 4). In a nonlinear system, a stationary incoherent wavepacket, that is a RPLS, can form if diffraction is exactly balanced by nonlinearity. In this section, we theoretically describe the characteristic properties of random-phase solitons in nonlinear periodic lattices. An RPLS is characterized by its intensity profile, power spectrum, statistical (coherence) properties, and by the structure of the coherent waves that describe it within the modal theory. All these quantities provide different information on the RPLS, but they are all intimately related. In order for a RPLS to exist, its intensity profile, power spectrum, coherence properties, and its coherent wave composition, must all conform to the lattice periodicity [37].

The behavior of the power spectra of RPLSs is perhaps the most interesting among all their features, and it can be described in an intuitive fashion by qualitatively analyzing the diffraction in periodic media. When the beam is incoherent, the width of its power spectrum may extend over a wide region in the \mathbf{k} -space [37, 45, 52]. As we have already discussed in the previous section, in \mathbf{k} -space, there are regions of normal and anomalous diffraction. Solitons occur when a stable balance is achieved between diffraction and nonlinearity. However, as nonlinear self-focusing balances normal diffraction, we intuitively conclude that in a self-focusing medium, the Floquet-Bloch power spectrum of an RPLS should be mainly supported within the normal diffraction regions of the \mathbf{k} -space. The opposite should occur for self-defocusing media: self-defocusing effects balance anomalous diffraction, and thus the Floquet-Bloch power spectra of RPLSs in a self-defocusing medium should be located primarily in the anomalous diffraction regions of the \mathbf{k} -space. We express the power spectra of an incoherent beam in terms of the Fourier transform,

$$J_{\text{FT}}(\mathbf{k}, z) = \sum_m d_m \left| \int d\mathbf{r} \psi_m(\mathbf{r}, z) e^{-i\mathbf{k}\cdot\mathbf{r}} \right|^2, \quad (12)$$

and by projecting the coherent waves onto the FB waves of the linear waveguide array,

$$J_{\text{FB}}(\mathbf{k}, z) = \sum_m d_m \left| \int d\mathbf{r} \psi_m(\mathbf{r}, z) f_{n\mathbf{k}}^*(\mathbf{r}) e^{-i\mathbf{k}\cdot\mathbf{r}} \right|^2; \quad (13)$$

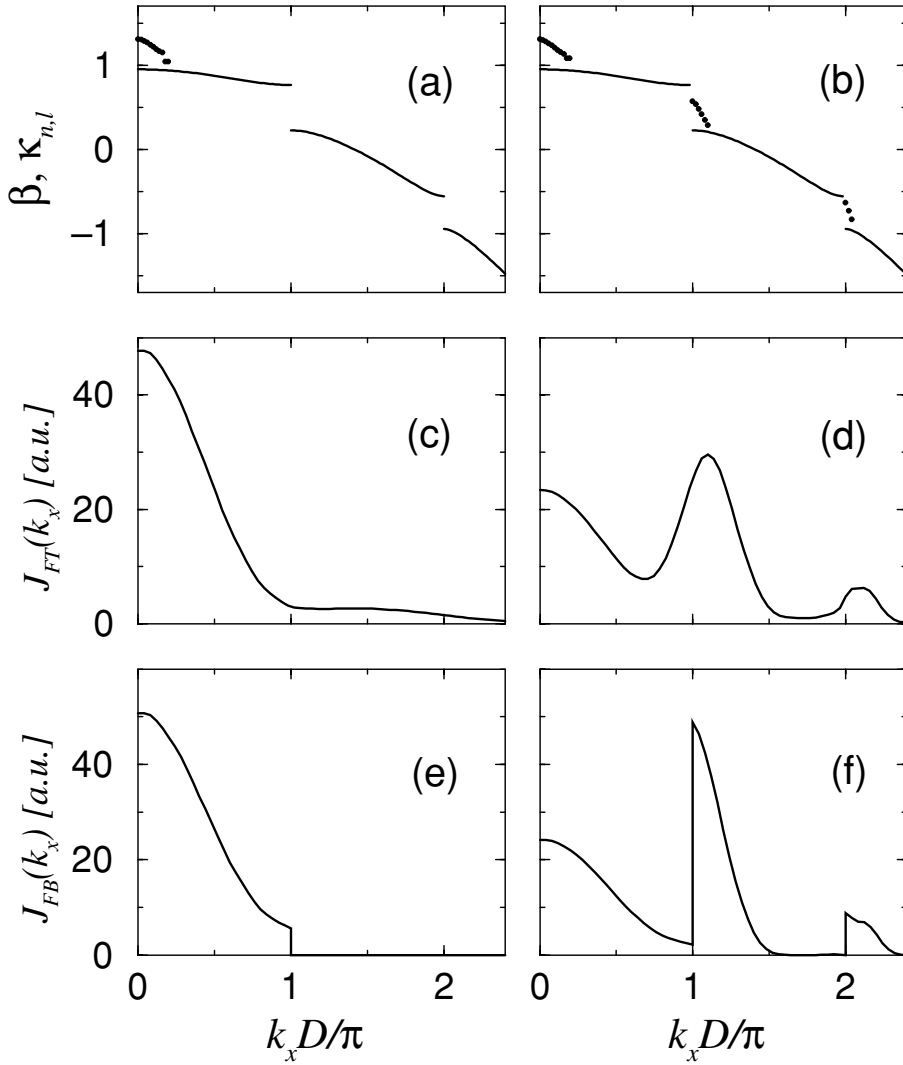


Figure 2. The propagation constants, and power spectra of the two examples of RPLSs. Diffraction curves $0.58kx_0^2\beta$ vs. $k_x D/\pi$ (solid curves) of the linear periodic system, and the propagation constants $0.58kx_0^2\kappa_{n,l}$ (circles) of (a) a 1st-band RPLS, and (b) a three-band RPLS. The Fourier power spectrum of (c) the 1st-band RPLS, and (d) the three-band RPLS. The power spectra in the FB basis for (e) the 1st-band soliton, and (f) the three-band soliton.

here \mathbf{r} denotes the transverse (1D or 2D) coordinate. The intuitive prediction above is verified numerically [37] and experimentally [45]. Figures 2(c)–(f) illustrate the power spectra of two RPLS examples calculated numerically in a 1D nonlinear periodic lattice with a self-focusing nonlinearity (for exact

parameters see below); the spectra are mainly located in the normal diffraction regions of the BZs.

All properties of RPLSs can be calculated from their coherent wave structure, which must be such that the self-consistency loop is closed: the incoherent beam (described by a set of coherent waves ψ_m) induces, via the nonlinearity, a defect in the periodic lattice $\delta n[I(\mathbf{r})]$. This defect in the lattice creates localized (defect) states, whose propagation constants reside in the gaps of the spectrum of the linear system. If some (or all) of the defect states are *identical* to the coherent waves ψ_m making up the incoherent beam, the self-consistency loop is closed, and the incoherent beam described by such jointly localized coherent waves is an RPLS. It is convenient to change the notation for the coherent waves of an RPLS: $\psi_m \rightarrow \psi_{n,l} = u_{n,l}(\mathbf{r})\exp(i\kappa_{n,l}z)$. In this notation, the propagation constant $\kappa_{n,l}$ of a coherent wave $\psi_{n,l}$ resides in the gap above the n th band (see circles in Figures 2(a) and (b)), while l describes the hierarchy within a single gap (if $l < l'$ then $\kappa_{n,l} > \kappa_{n,l'}$). Mathematically, a closed self-consistency loop means that the spatial profiles $u_{n,l}(\mathbf{r})$ are eigenmodes, and the propagation constants $\kappa_{n,l}$ are the corresponding eigenvalues, of a nonlinear eigenvalue equation,

$$\frac{1}{2\kappa} \nabla^2 u_{n,l} + \frac{\{p(\mathbf{r}) + \delta n[I(\mathbf{r})]\} \kappa}{n_0} u_{n,l} = \kappa_{n,l} u_{n,l}(\mathbf{r}), \quad (14)$$

where

$$I(\mathbf{r}) = \sum_{n,l} d_{n,l} |u_{n,l}(\mathbf{r})|^2. \quad (15)$$

The localized eigenmodes $\psi_{n,l}$ are randomly excited; their time-averaged occupancy is given by the modal weights $d_{n,l}$. The statistical properties of RPLSs described above are stationary during propagation because $B(\mathbf{r}_1, \mathbf{r}_2) = \sum_{n,l} d_{n,l} u_{n,l}(\mathbf{r}_1) u_{n,l}^*(\mathbf{r}_2)$ is independent of z , $\partial B(\mathbf{r}_1, \mathbf{r}_2)/\partial z = 0$.

In the qualitative analysis above we have implicitly assumed that the defect in the periodic lattice, induced by RPLS via nonlinearity, does not severely alter the lattice at the position of RPLS. For example, the maximal index change due to nonlinearity is, say, less than 50% of the lattice depth. Furthermore, we have implicitly assumed that the width of the gap just below the first band is not significantly larger than the width of the first band itself (the lattice is not too deep); in this case diffraction effects are more pronounced, and diffraction lengths are smaller.

The analysis of RPLSs above is applicable to both (1+1)D and (2+1)D solitons, and various types of nonlinear media. In what follows, we outline results related to the intensity structure and the coherence properties of (1+1)D RPLSs in self-focusing and saturable nonlinear medium, $\delta n(I) = \gamma I / (1 + I/I_S)$. Most of these results are expected to hold in a more general setting. The periodic potential used in the calculation is $p(x) = p_0 \sum_m \exp -[(x - mD)/x_0]^8$, while the parameters are $n_0 = 2.3$,

$p_0 = 4 \cdot 10^{-4}$, $x_0 = 3.7 \mu\text{m}$, $D = 10 \mu\text{m}$, $k = n_0 2\pi/\lambda$, where $\lambda = 488 \text{ nm}$, and $\gamma I_S = 1.5 \times 10^{-4}$. We present two RPLS examples where the localized modes $u_{n,l}$ originate (1) solely from the first band and (2) from the first three bands. The power is distributed among the localized modes as $d_{n,l} \propto \exp[-l^2/(2w_n^2)]$ for $l \leq l_n$, where l_n denotes the number of excited modes in the gap above the n th band. For the 1st-band RPLS $l_1 = 11$, $w_1 = 4.34$ (Figures 3(a) and (b)), while for the three-band RPLS $l_1 = 11$, $l_2 = 6$, $l_3 = 3$, $w_1 = 4.34$, $w_2 = 2.36$, and $w_3 = 3.55$ (Figures 3(c)–(f)). The propagation constants of the 1st-band RPLS are all located in the semi-infinite gap above the first band (see circles in Figure 2(a)). The propagation constants of the three-band RPLS are located in three gaps (see circles in Figure 2(b)).

The self-induced defects of the RPLSs are broad due to the fact that a number of defect modes (coherent waves $\psi_{n,l}$) are excited (e.g., see Figure 3(f)). The defect structure depends on the intensity of the RPLS. The envelopes of the intensity profiles of RPLSs are generally broad and cover several lattice sites (waveguide channels). Notice the (spatial) intensity oscillations superimposed on the envelopes, conforming to the periodicity of the lattice. The structure of these oscillations depends on the structure of the coherent waves $\psi_{n,l}$. For example, when all the coherent waves $\psi_{n,l}$ originate from the 1st-band (i.e., when all propagation constants $\kappa_{n,l}$ are in the semi-infinite gap), then the intensity is mainly localized on-sites (within the waveguides; see Figure 3(a)). However, when there is considerable amount of power in the coherent waves $\psi_{n,l}$ originating from higher bands, then a larger amount of power is also found in the interstitial regions (Figure 3(c)).

This is explained by observing (in our numerical simulations) that the self-localized coherent waves of an RPLS inherit the properties of the FB waves from which they originate [30, 37]. The extended FB waves from higher bands have a larger amount of power in the interstitial regions; the same holds for the self-localized RPLS modes that originate from these bands. In addition, we have numerically observed that the self-localized modes originating from the n th band are orthogonal with the extended FB waves from other bands. Thus, the FB spectrum of the 1st-band RPLS is entirely located within the 1st BZ [37].

Let us now discuss the (statistical) coherence properties of an RPLS. The correlation between randomly fluctuating fields $E(x, z, t)$ at points x_1 and x_2 from the same transverse plane z is expressed by the complex coherence factor, $\mu(x, x') = B(x, x')/\sqrt{I(x)I(x')}$. The spatial correlation distance $l_s(x) = \int_R dx' |\mu(x, x')|^2$ expresses the length scale at which there is still some correlation between the fluctuating fields; the region of integration R is several times larger than the soliton region. A commonly observed feature of RPLSs is that, within a (broad) soliton region, the statistical properties of an RPLS are approximately invariant under translations by a lattice constant,

$$\mu(x, x') \approx \mu(x + D, x' + D), \quad (16)$$

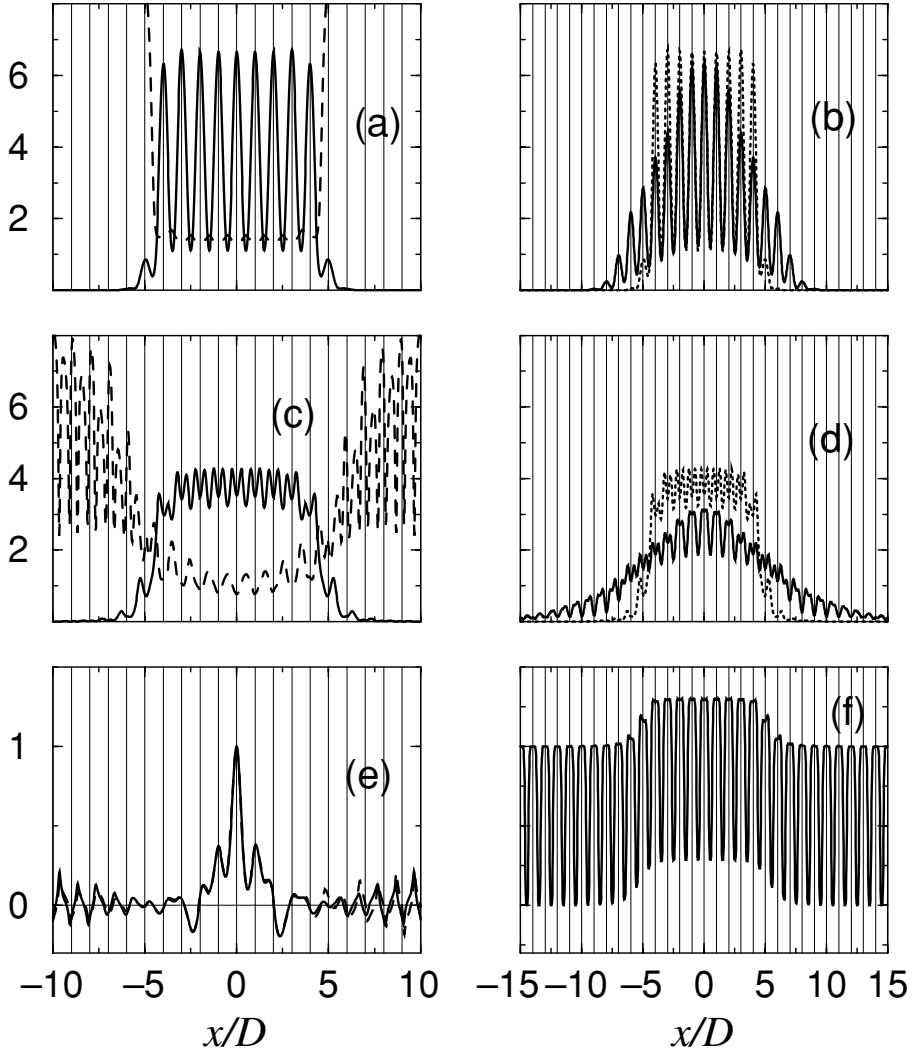


Figure 3. The intensity profiles, diffraction, and spatial coherence properties of the RPLSs. First-band RPLS: (a) the intensity profile $I(x)/I_S$ (solid line) and $l_s(x)/D$ (dashed line); (b) diffraction after 8.29 mm of propagation. Three band RPLS: (c) $I(x)/I_S$ (solid line) and $l_s(x)/D$ (dashed line); (d) diffraction after 8.29 mm. (e) The complex coherence factors $\mu(x, 0)$ (solid line) and $\mu(x + D, D)$ (dashed line) of the three-band RPLS; the two graphs are almost identical. (f) The normalized induced potential $V(x)$ (defect) of the three-band RPLS containing the periodic and nonlinear term. Vertical lines denote the lattice sites.

which is illustrated in Figure 3(e). As a consequence of that, the spatial correlation distance behaves periodically within a soliton region, $l_s(x) \approx l_s(x + D)$ (see Figures 3(a) and (c)). From Figures 3(a) and (c) we also see that the spatial correlation distance increases at the tails of the RPLS, which

is explained by noting that only the slowly decaying modal constituents are present at the tails, which increases the spatial coherence in that region. The same feature is observed for incoherent solitons in homogeneous media [67].

To check whether a solution is indeed an incoherent soliton, we have to check its stability against small perturbations, and study the diffraction of such a beam when the nonlinearity is turned off. The diffraction characteristics of our RPLSs examples are shown in Figures 3(a) and (d). The diffraction of an incoherent beam as a whole depends on the direction of propagation and diffraction coefficients associated with each coherent wave $\psi_{n,l}$ (Section 4).

6. Random phase lattice solitons: Experiments

According to the theoretical prediction, the properties of an RPLS are complex, e.g., the power spectrum should be multihumped, with humps being located at normal (anomalous) diffraction regions of the \mathbf{k} -space in the case of self-focusing (defocusing) nonlinearity. To experimentally observe an RPLS, ideally, an incoherent beam with the properties of an RPLS should be first engineered, and then launched into a nonlinear waveguide array to check whether it is truly a soliton. Unexpectedly, we experimentally found that a probe beam with a homogeneous \mathbf{k} -space distribution (displaying a single hump with a proper width) and a bell-shaped intensity structure self-adjusts its spectrum and intensity structure and evolves naturally, under proper nonlinear conditions, into an RPLS [45]. Figure 4(b) shows the homogeneous power spectrum of the input beam, which has evolved into a multihumped power spectrum of an RPLS shown in Figure 5(e); the nonlinearity is of the self-focusing type, hence, the humps are in the regions of the normal diffraction (see text below for details). This finding of the evolution of an incoherent

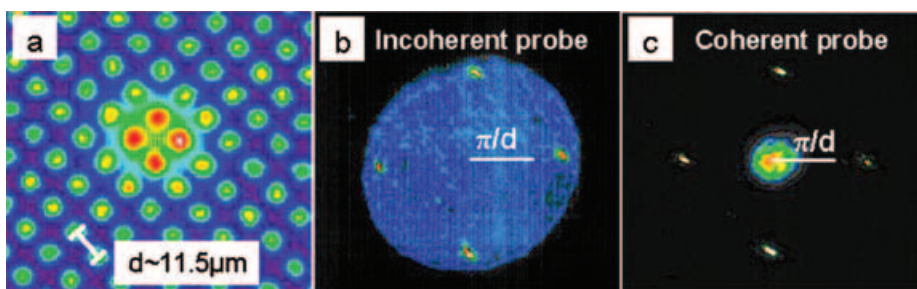


Figure 4. The properties of the incoherent input beam at the input face of a nonlinear photonic lattice. (a) The induced square lattice and the incoherent input beam in real space; the lattice spacing is $11.5 \mu\text{m}$. (b) Wide circle shows the Fourier power spectrum of the incoherent input; four dots are the power spectra of the lattice-forming beams; they define the corners of the first Brillouin zone. (c) The Fourier power spectrum of a coherent beam with the same intensity envelope as the incoherent input beam from (a).

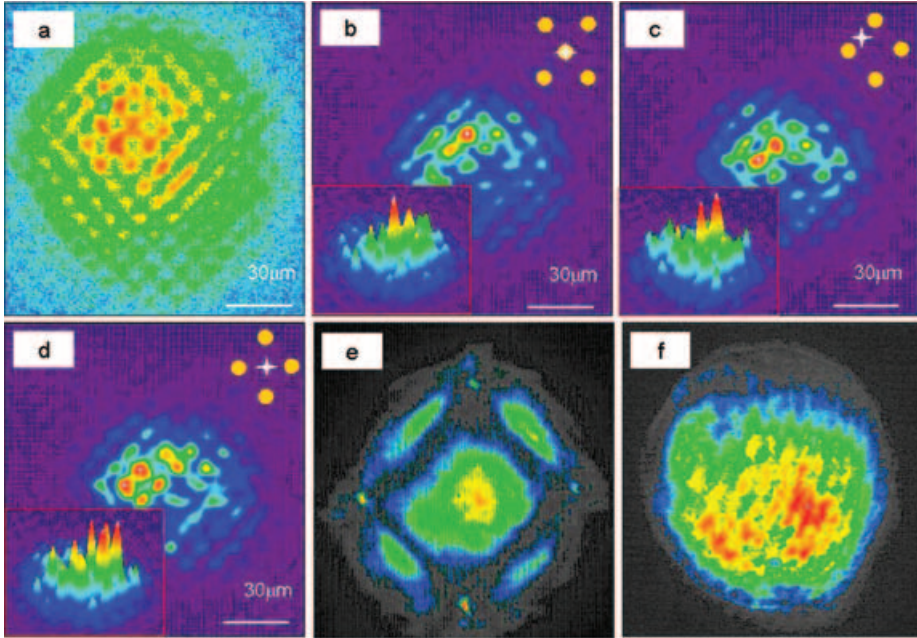


Figure 5. The properties of the incoherent beam (RPLS) after it propagates through the nonlinear medium. (a) Diffraction of an incoherent beam with low intensity; other properties are identical to the input beam from Figure 4. Pictures of the RPLSs in real space: (b) centered on-site, (c) centered between two lattice sites (waveguide arrays), and (d) centered between four lattice sites. Note that the diffracted beam from (a) has ~ 2.5 times larger width than the RPLSs. (e) Picture representing the RPLSs in Fourier space. The power spectrum is multihumped with square symmetry. The humps are located in the normal diffraction regions of the first two Brillouin zones (four dots represent the corners of the first Brillouin zone). (f) The Fourier power spectrum of an incoherent beam after it propagates through a homogeneous nonlinear medium (the lattice is removed); the multi-humped features do not exist.

input beam with a simple structure toward a RPLS indicates that the nonlinear dynamics of partially coherent waves in nonlinear periodic systems possesses many intriguing features that merit further exploration.

The source of the quasimonochromatic partially spatially coherent light is in our experiments constructed by sending a 488-nm laser beam through a rotating diffuser, and then 1:1 imaging the beam exiting the diffuser with a telescopic 4f system onto the input face of the crystal (Figure 6). The coherence time of the light can be controlled by the rotation rate of the diffuser, while the degree of spatial coherence and the power spectrum of the exciting beam (the probe beam) can be controlled by a spatial filter in the Fourier plane of the 4f system (Figure 6).

Our experiments are carried out in optically induced nonlinear photonic lattices [24], previously used to demonstrate lattice solitons in both one and two dimensions [26, 27]. As the induction technique is essentially holographic, the method can be used to construct lattices of arbitrary geometry (e.g., square,

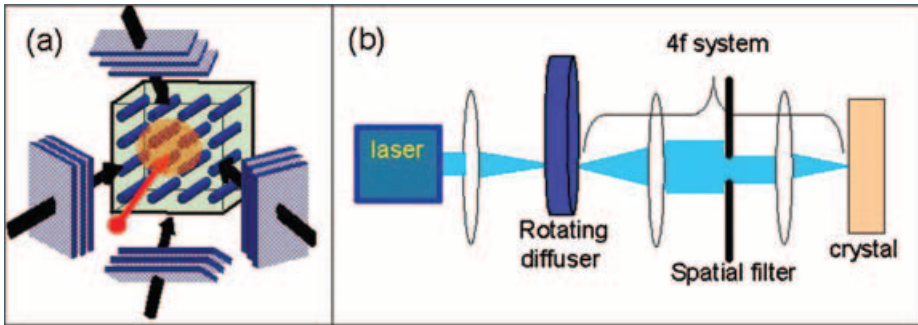


Figure 6. The experimental setup. (a) The schematic picture of the setup used to obtain the two-dimensional, square, nonlinear photonic lattice. (b) The schematic picture which shows the setup used to construct a partially spatially incoherent source. The width of the power spectrum (and hence the degree of coherence) can be controlled with the spatial filter in the Fourier plane of the telescopic 4f system.

hexagonal, etc.). Here, we interfere plane waves in a photorefractive SBN crystal to obtain a 2D square array of 2D waveguides (see Figure 4(a) and 6). The nonlinearity results from the photorefractive screening effect [50]. The strength of the nonlinearity is controlled by voltage applied across the crystalline c -axis [50]. For the experiments described here, the lattice is 5-mm long, each array beam has 15 mW of power, and the nonlinearity is set by applying 1 kV across the crystal. We note that the nonlinear response time of the medium is much longer than the characteristic time of the random fluctuations of the incoherent beam; hence, the theoretical model described above is applicable in this system.

The characteristics of the input beam (the beam entering the nonlinear waveguide array) and the output beam (the beam exiting the nonlinear medium) are measured both in real space and in \mathbf{k} -space (for the latter we use a lens and monitor the intensity at the focal plane). This is important for the unambiguous interpretation of the results. The characteristics of the input beam are shown in Figures 4(a) and (b). Figure 4(a) depicts a real-space photograph of a probe beam ($26 \mu\text{m}$ at FWHM) launched into the induced square lattice (lattice spacing is $11.5 \mu\text{m}$). The probe beam is broad and covers several waveguide channels. Figure 4(b) shows the Fourier power spectrum of the incoherent probe beam (wide circle). The four dots in Figure 4(b) represent the Fourier power spectra of the lattice-forming waves. By construction, these lattice writing beams form Bragg angles in our system; hence, the corresponding square defined by the four dots in Figure 4(b) outlines the first BZ. The power spectrum of the incoherent input beam covers all of the first BZ and significant parts of the second BZ. It should be emphasized that the power spectrum of an incoherent beam depends not only on its envelope (as is the case for coherent beams), but also on the degree of coherence as well. For example, Figure 4(c) shows the power spectrum of a coherent input beam (with the diffuser removed)

of the same envelope in real space as the incoherent input beam. We see that the width of the power spectrum of the coherent beam is roughly three times smaller than the spectral width of the incoherent input beam. From this we infer that the average speckle size in the incoherent beam is less than one-third of the size of the envelope. Because the diameter of the envelope is equal to roughly three lattice spacings (see Figure 4(a)), the spatial correlation distance of this partially coherent beam is, therefore, comparable to the lattice period.

The incoherent beam is focused into the lattice with the real-space distribution and power spectrum shown in Figures 4(a) and (b), respectively. Figure 5 shows the characteristics of the beam at the output face of the crystal (i.e., after it propagates for 5 mm through a nonlinear lattice). Figure 5(a) shows diffraction for a probe beam with low-intensity, characterized by a 1:50 intensity ratio between the probe and array beams. The size of the output beam is about 2.5 times larger than the size of the input beam. For a 10 times larger intensity of the probe beam (1:5 ratio), the nonlinearity becomes strong enough to balance diffraction, and the incoherent probe beam self-traps and forms a random-phase lattice soliton. Figure 5(b) shows an RPLS centered on a site, while Figures 5(c) and (d) show RPLSs centered between 2-sites and 4-sites, respectively. Figure 5(e) depicts the power spectrum of the RPLSs. The M-symmetry points at the corners of the first BZ are defined by the four dots (spectra of the lattice-forming beams). The power spectrum of the RPLSs takes on the square symmetry of the lattice and is clearly multihumped. For this particular example, the nonlinearity is of the self-focusing type, thus the power spectrum is located within the normal diffraction regions of the first two BZs. When the lattice is removed, and all other parameters of the system kept fixed (applied bias field and intensity), the diffraction of the beam in such homogeneous (no lattice) medium is too strong to be fully balanced by the nonlinearity. Figure 5(f) shows the power spectrum of the output beam which is, unlike the RPLS spectrum, homogeneous.

In [45] we have also experimentally observed that an input beam with a homogeneous power spectrum covering only a part of the first BZ may evolve into an RPLS possessing a spectrum in the first two BZs. This indicates that power has moved from the anomalous diffraction regions of the first BZ to the normal diffraction regions of the second BZ. The dynamics observed in our experiments, namely, the evolution of an incoherent beam with bell-shaped intensity and power spectrum into an RPLS, is studied numerically in the next section.

7. Dynamical evolution of an input incoherent beam into a RPLS

In linear dynamical systems, one can project the initial excitation onto the orthogonal modes of the system, and observe the dynamics through linear superposition. The energy present in every orthonormal mode is conserved

during evolution. However, even a small nonlinearity added to the system can induce energy transfer between the modes of the linear system. This fact has motivated Fermi, Pasta, and Ulam to study the dynamics in a nonlinear lattice, and investigate the possibility of thermalization via nonlinearity [80]. They expected that, when just one or a few modes of the linear system are initially excited, the nonlinearity would transfer the energy to other modes and lead to the equipartition of energy (uniform distribution of energy among all linear modes). They have discovered that instead of thermalization, the system cycles in an almost periodic fashion, while energy recurs to the initial mode [80]. In our experimental study of RPLSs, it turned out that the nonlinear transfer of energy among the modes of the linear system can be exactly such that, under proper nonlinear conditions, a homogeneous \mathbf{k} -space excitation evolves into characteristic multihumped shape of an RPLS. Thus, the initial condition is in a sense opposite to that of the famous FPU work [80]. Here we roughly homogeneously excite a large number of modes of the linear system, yet the energy redistributes and eventually evolves into an inhomogeneous distribution with the characteristic RPLS shape. This fascinating experimental observation motivated us to study the physics underlying such nonlinear evolution process. As a representative example, we study the evolution of a beam with a bell-shaped intensity structure and a bell-shaped statistics, for example, a beam of light from a Gaussian–Schell source [78]. Such an input beam will dynamically evolve in a nonlinear waveguide array and change its intensity structure and the power spectrum depending on the properties of the lattice and the nonlinearity. In this section, we show theoretically that, indeed, a beam with a bell-shaped intensity structure and power spectrum may, under proper nonlinear conditions, evolve into a beam with the characteristic RPLS properties.

7.1. Evolution in a (1 + 1)D system

We start the analysis in a 1D geometry. The modal structure of an incoherent beam with the bell-shaped intensity structure and a bell-shaped Fourier power spectrum may be written as

$$\psi_{k_x}(x, z = 0) = \sqrt{I_0(x)}G(k_x)e^{ik_x x}, \quad (17)$$

where $I_0(x)$ is the intensity structure of the beam at $z = 0$. For the clarity of the exposition, in this subsection we have changed the notation for coherent waves: $\psi_m \rightarrow \psi_{k_x}$; k_x is a real continuous variable that has a physical meaning of the transverse momentum of the k_x th mode, while $G(k_x)$ is a real function defining the weight of the k_x th mode; $G(k_x)$ is normalized so that $\int dk_x |G(k_x)|^2 = 1$. The initial mutual coherence function of such a beam follows from Equation (5),

$$B(x_1, x_2, 0) = \sqrt{I_0(x_1)I_0(x_2)} \int_{-\infty}^{\infty} |G(k_x)|^2 e^{ik_x(x_1-x_2)} dk_x. \quad (18)$$

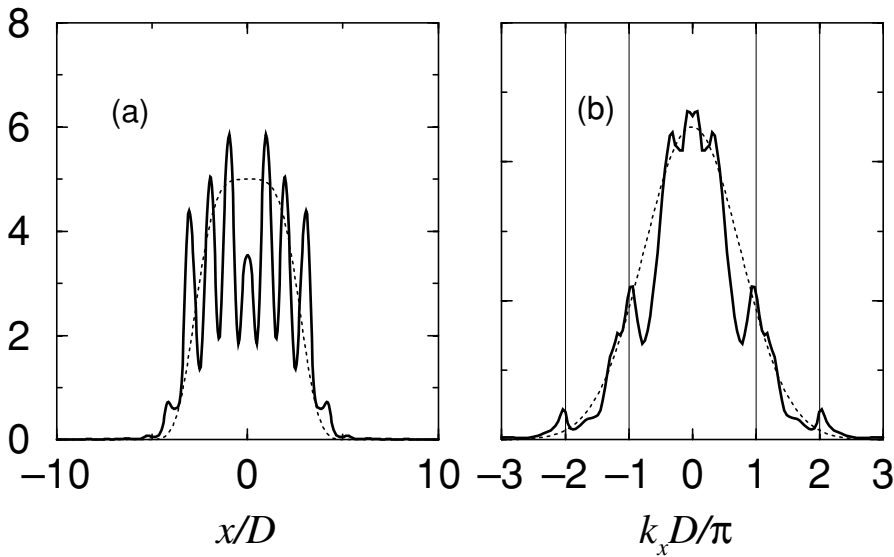


Figure 7. (a) The intensity structure and (b) the power spectra of the beam at the input face of the medium (dotted lines), and after the evolution through the nonlinear medium (solid lines). Vertical lines in (b) denote the edges of the Brillouin zones.

The coherence properties are obviously contained solely within the function $G(k_x)$; if this function is broader, the transverse momentum spread is larger and the input beam is more incoherent.

In Section 5, we have self-consistently calculated a $(1+1)$ D RPLS and analyzed their properties. Let us return to that particular system (with exactly the same parameters of the lattice and the nonlinearity). Consider an incoherent beam with the intensity structure and spatial statistics given by $I_0(x) = I_p \exp[-(x/I_w)^4]$, $I_p = 5I_S$, $I_w = 3D$, $G(k_x) = G_0 \exp[-(k_x/k_w)^2]$, $k_w = 1.5\pi/D$, G_0 is set so that $\int dk_x |G(k_x)|^2 = 1$. The bell-shaped intensity structure and the Gaussian-like Fourier power spectrum of this input beam are shown in Figure 7 with dotted lines. The intensity profile of the input beam covers roughly five to seven waveguide arrays, while its power spectrum covers all of the first BZ, and a large portion of the second BZ. Such a beam is launched into a nonlinear waveguide array and its propagation dynamics is simulated with a standard split-step Fourier technique. The evolution of the intensity structure and the power spectrum are shown in Figures 8 and 9, respectively. We observe the following: In the initial stages of the evolution, the beam self-adjusts to conform to the periodicity of the lattice; during this brief initial stage a small amount of power is radiated away from the beam. After this brief initial stage the beam stays self-trapped for many diffraction lengths; it does not change its width and covers about seven waveguides (Figure 8). The evolution of power spectrum is the most interesting. The power

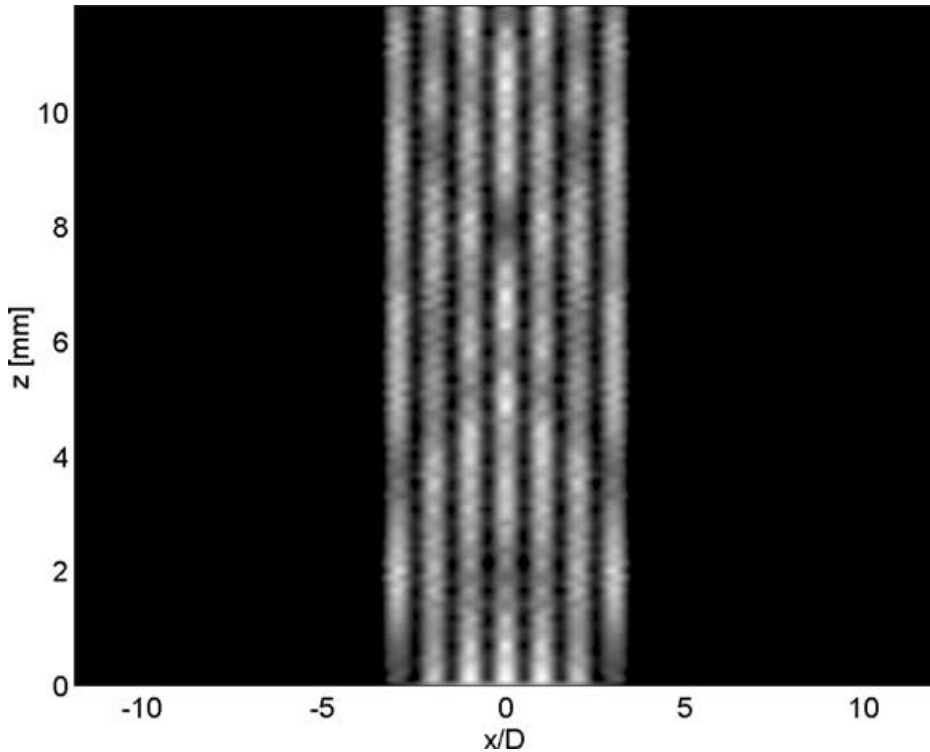


Figure 8. Evolution of the intensity profile of an incoherent beam in a $(1+1)D$ nonlinear waveguide array. The beam is self-trapped and evolves for many diffraction lengths without broadening; the width of the beam is covering seven waveguide arrays.

spectrum evolves in such a way to become multihumped, with humps being located in the normal diffraction regions of the first two BZs (Figure 9); a very small amount of power is located also in the third BZ, close to its edges in the normal diffraction region. Solid lines in Figure 7 illustrate the intensity structure and the power spectrum of the beam at the output. Small internal oscillations in the structure of the beam that are present during the evolution are attributed to the fact that the beam dynamics corresponds to a trajectory in a phase space that is not an exact soliton solution. However, due to the fact that the beam is self-trapped, and its width is not changed for many diffraction lengths, we conclude that this trajectory runs close to an exact solitary wave, such as the one calculated in Section 5.

To verify that the characteristic evolution of the bell-shaped input beam (both in real and Fourier space) shown in Figures 8 and 9 is indeed a nonlinear effect, rather than just a result of the lattice periodicity, we simulate the evolution of the intensity structure of exactly the same input beam, in identical periodic system, but with nonlinearity turned off. The results are shown in Figure 10, which clearly displays the absence of self-trapping, i.e., the beam diffracts.

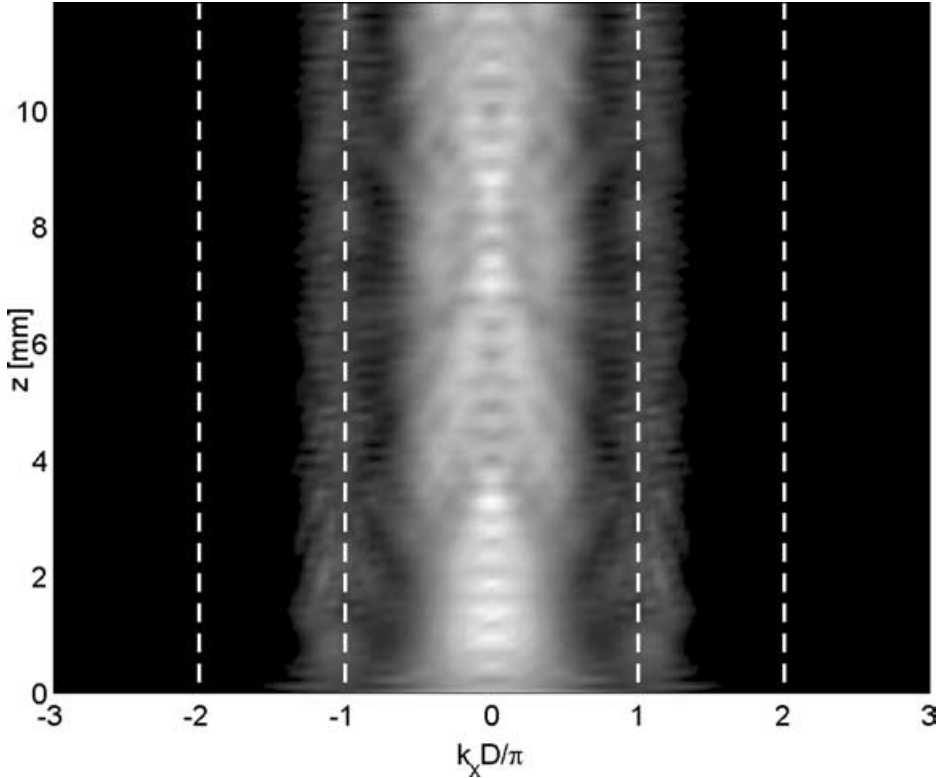


Figure 9. Evolution of the Fourier power spectrum of an incoherent beam in a (1+1)D nonlinear waveguide array. The initial Gaussian-like power spectrum becomes multihumped, with humps being located mainly in the normal diffraction regions of the first two Brillouin zones.

7.2. Evolution in a (2+1)D system

Previous numerical simulations in 1D models have shown that an incoherent beam with initially simple structure of the intensity and the power spectrum may, under proper nonlinear conditions, evolve into a beam with characteristics of an RPLS, e.g., with multihumped power spectrum. However, the experimental study of this system was performed in a (2+1)D photonic lattice, which motivates us to study the evolution of an incoherent beam in a (2+1)D model. The experiment was performed in an optically induced lattice in a photorefractive SBN:75 crystal, where the potential $V(\mathbf{r}, z)$ from evolution equations (4) and (6) has the form

$$V(\mathbf{r}, z) = -\frac{1}{2}n_e^3 r_{33} V W^{-1} \left[1 + \frac{I_l(\mathbf{r})}{I_b} + \frac{I_p(\mathbf{r}, z)}{I_b} \right]^{-1}. \quad (19)$$

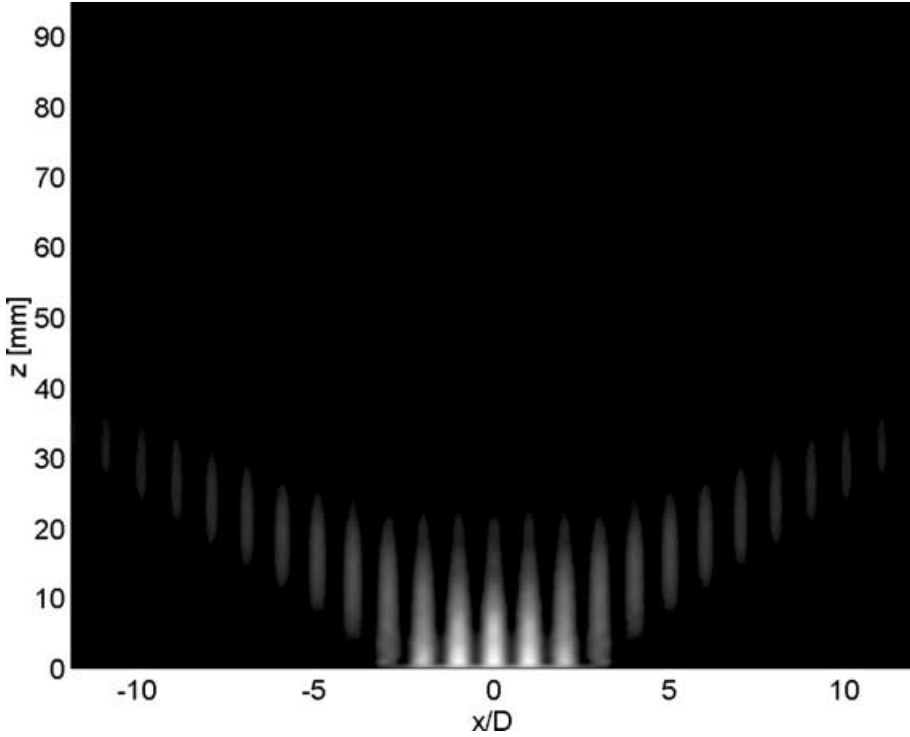


Figure 10. Linear dynamics (diffraction) of an incoherent beam in a lattice; input intensity structure and other properties are identical to the beam from Figure 8.

In our system, $n_e = 2.3$ is the linear index of refraction, $r_{33} = 1022 \text{ pmV}^{-1}$ is the electro-optic coefficient, $W = 6 \text{ mm}$ is the transverse width of the crystal; the wavelength of the light is 488 nm in vacuum; $I_l(\mathbf{r})$ denotes the intensity of the lattice-forming beams, $I_p(\mathbf{r}, z)$ is the intensity of the probe, while I_b is the intensity of the background illumination. The voltage V applied across the crystalline c -axis can be used to control the strength and the sign of the nonlinearity [45].

The photonic square lattice is formed by interfering four plane waves; the intensity structure of the lattice-forming beams is of the form $I_l(\mathbf{r}) = I_{l0}[\cos(x - y)\pi/D - \cos(x + y)\pi/D]^2$, where the lattice constant is $D = 11.5 \mu\text{m}$; the peak intensity of the lattice beams is $I_{l0} = 0.28I_b$, while the peak intensity of the input (probe) beam is $I_{p0} = 0.15I_b$. The voltage is set to 780 V . The input beam has a Gaussian intensity structure, and a Fourier power spectrum, which roughly homogeneously covers a circle with radius of approximately $1.5\pi/D$ (Figure 11). Thus, all of the first BZ, and a large portion of the second BZ are excited. Figures 12 and 13 depict the evolution of the intensity structure and the Fourier power spectrum, respectively, at four equally

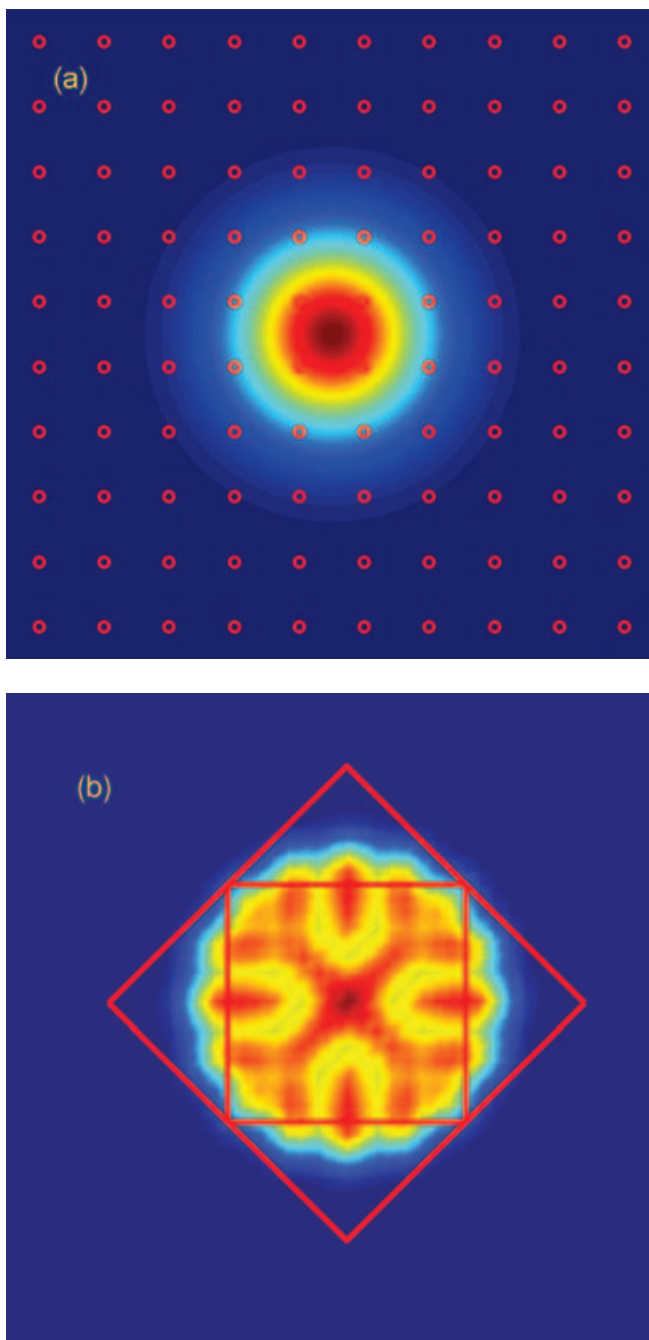


Figure 11. (a) The intensity structure and (b) the power spectra of a two-dimensional incoherent beam at the input face of the medium. For comparison, (c) shows the Fourier power spectrum of a fully coherent beam with the same intensity structure. Solid lines in (b) and (c) depict the edges of the first two Brillouin zones.

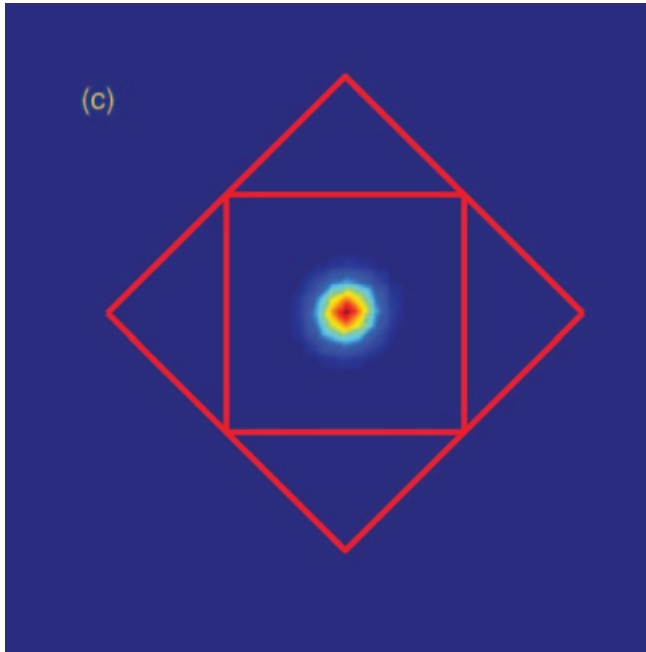


Figure 11. Continued.

spaced positions along the propagation axis: (a) $z = 5$, (b) 10, (c) 15, and (d) 20 mm. Clearly, the input Gaussian intensity structure from Figure 11(a) has evolved into an RPLS intensity structure, that covers four lattice sites with a large amount of the intensity, and six adjacent lattice sites with a bit less intensity (see Figure 12(d)). During the initial transient stage of the evolution, the beam has self-adjusted its properties and conformed its intensity structure and the Fourier power spectrum with the lattice periodicity. A small amount of power was radiated from the beam during this process. However, after this transient period, the beam stays self-trapped, and evolves as a solitary wave. Again, the evolution of power spectrum is the most interesting. Power is transferred from the anomalous diffraction regions of the 1st BZ into the normal diffraction regions of the 2nd BZ, so that the acquired power spectrum has a characteristic RPLS multihumped shape (Figure 13). When the nonlinearity is turned off, an identical input beam diffracts, and stationary propagation does not occur.

The numerical simulations discussed above show that one can obtain self-trapped (stationary) beam evolution even with a beam that initially has a simple structure in real and in Fourier space. The physical mechanism behind this is the fact that nonlinearity transfers the energy between the modes of a linear system. While the details behind this energy transfer are still under

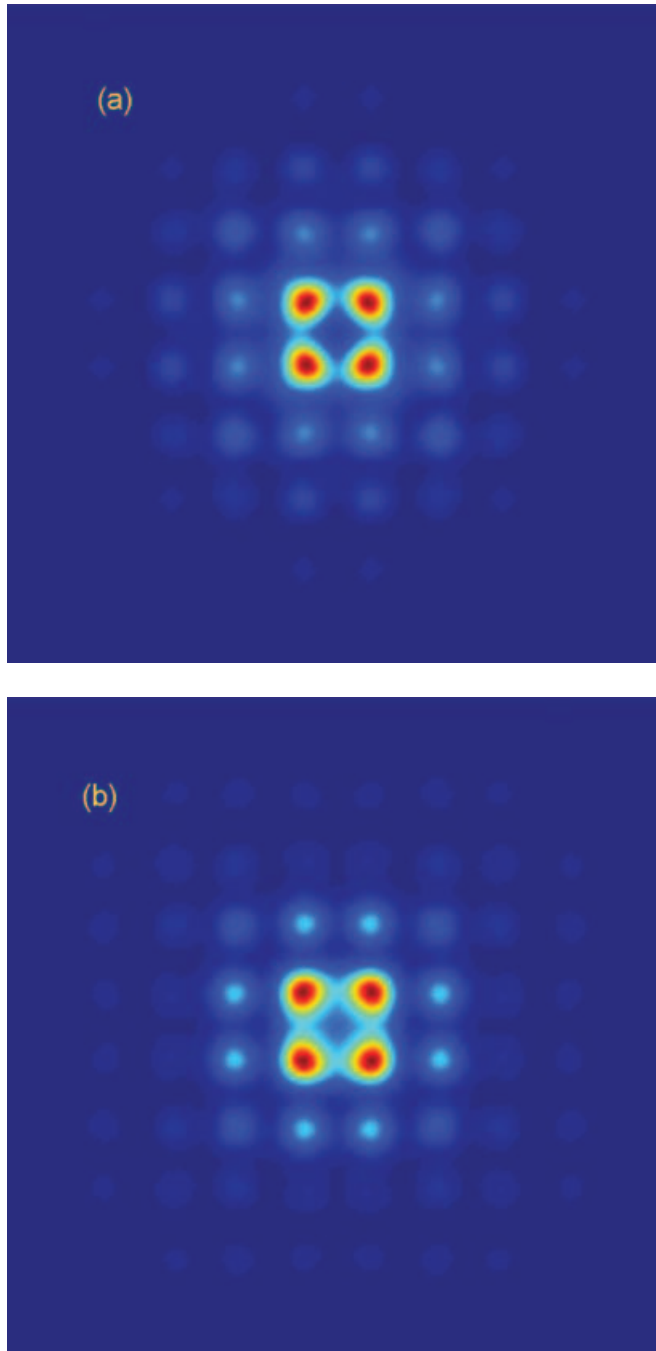


Figure 12. Propagation of the intensity profile of an incoherent beam in a $(2+1)$ D nonlinear waveguide array. The beam is self-trapped and evolves for many diffraction lengths without broadening; the beam covers $4+6$ lattice sites (waveguide arrays).

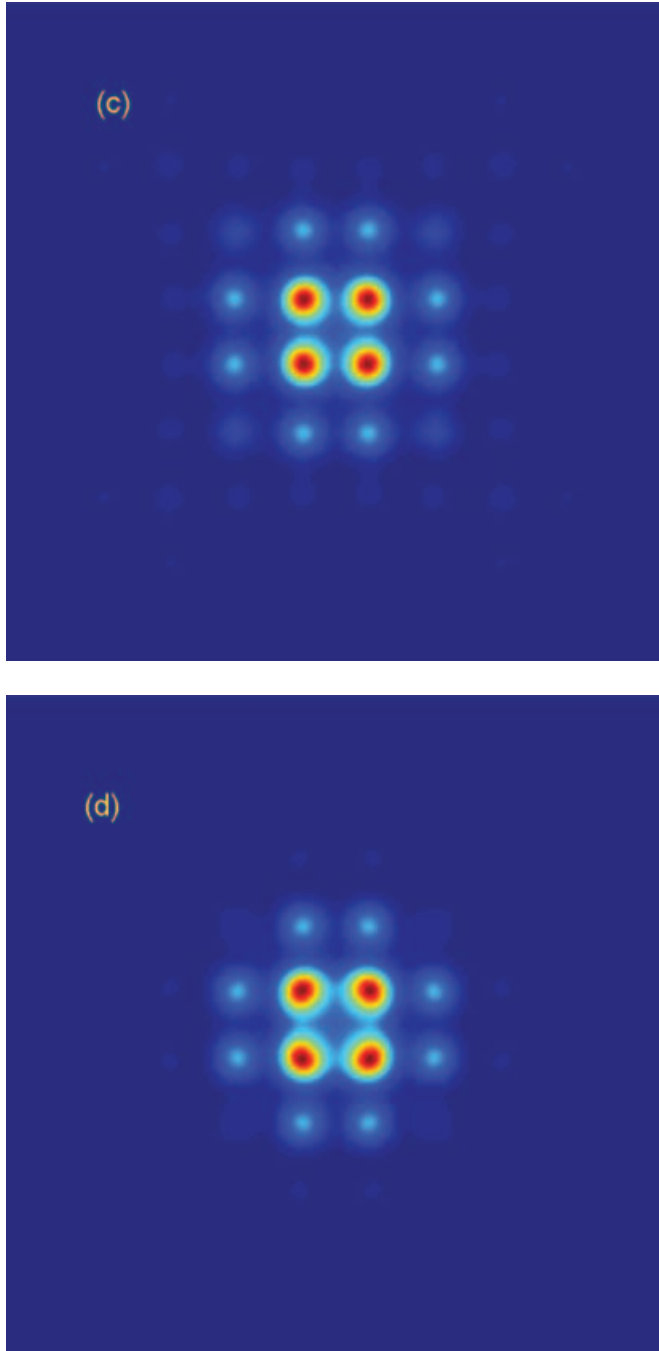


Figure 12. Continued.

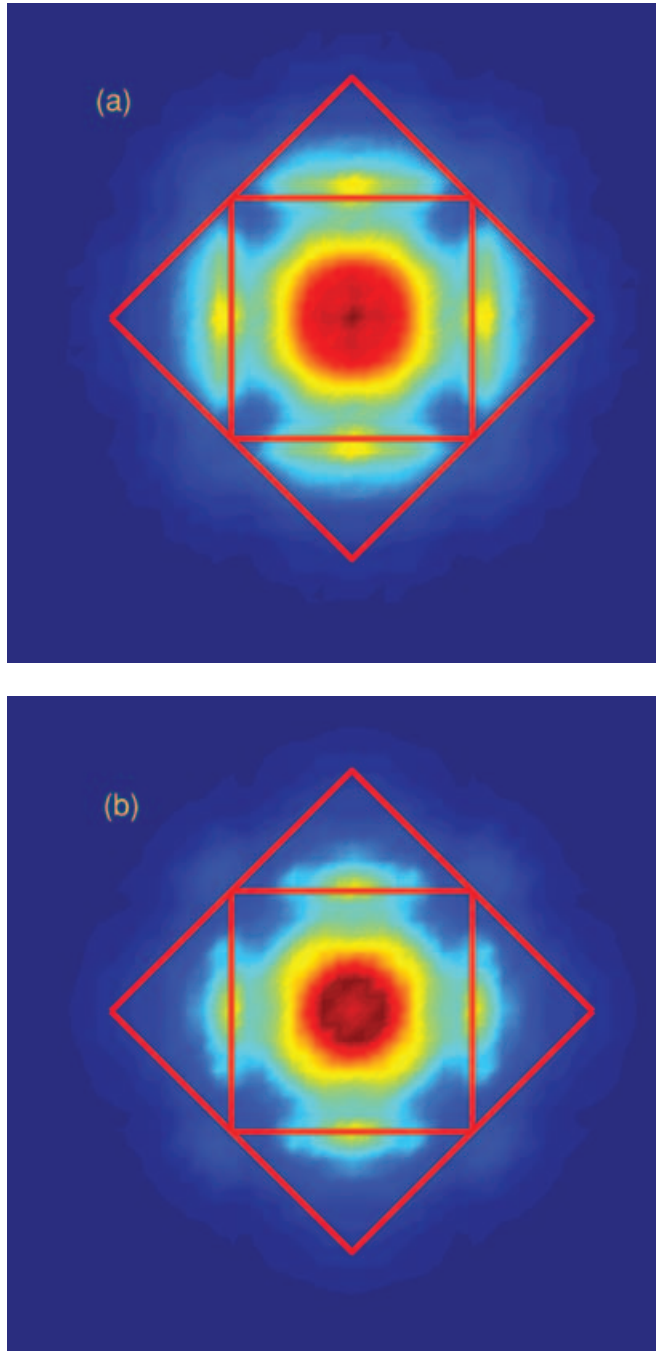


Figure 13. Evolution of the Fourier power spectrum of an incoherent beam in a $(2+1)D$ nonlinear waveguide array. The initial roughly homogeneous power spectrum from Figure 11(b) becomes multihumped, with humps being located mainly in the normal diffraction regions of the first two Brillouin zones (see text).

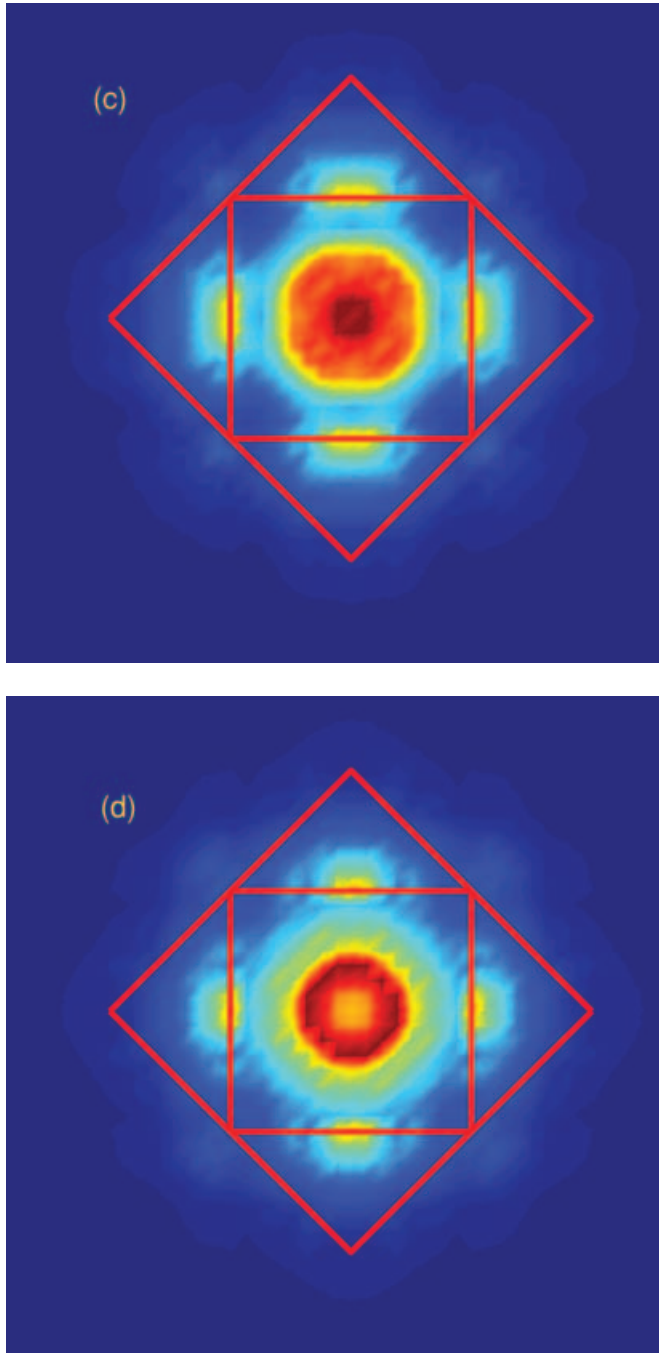


Figure 13. Continued.

investigation, it has been experimentally demonstrated that these ideas can be further developed to obtain a novel experimental technique for the BZS of nonlinear photonic lattices [46].

8. Conclusion

In conclusion, we have studied the propagation of partially coherent waves in nonlinear periodic systems. This problem is universal and appears in various contexts, such as partially condensed Bose gases in optical lattices (partially coherent matter waves), temporally incoherent waves in photonic crystals, etc. In this paper we have focused on recent theoretical [37] and experimental results [45] related to partially coherent solitary waves in nonlinear waveguide arrays. It was demonstrated that for these solitons to exist, the properties of the incoherent light, that is, intensity, power spectra, and coherence (statistical) properties, must conform to the lattice periodicity. In particular, it has been shown, theoretically and experimentally, that the power spectra of RPLSs should be mainly located in the normal (anomalous) diffraction regions of the BZs in case of self-focusing (defocusing) nonlinearity. Furthermore, the experiment has shown that an input incoherent beam with simple bell-shaped intensity structure and power spectrum may (under proper nonlinear conditions) naturally evolve into an RPLS exhibiting its complex intensity structure and power spectrum. The new result presented here is the theoretical study of this type of evolution in both $(1 + 1)$ D and $(2 + 1)$ D geometries, which underpins the experimental results on RPLSs. The transformation of a bell-shaped power spectrum into a multihumped RPLS-like power spectrum is allowed by the proper type of energy transfer between the modes of the linear system, which occurs when suitable nonlinear conditions are met. All these examples highlight the fact that partially coherent waves propagating in nonlinear periodic structures are fundamentally intriguing and rich dynamical systems. The progress on the experimental front holds much potential for applications. In particular, the studies presented here opened the way for a novel experimental technique of BZS [46].

References

1. A. S. DAVIDOV, Solitons and energy-transfer along protein molecules, *J. Theor. Biol.* 66:377–387 (1977).
2. W. P. SU, J. R. SCHIEFFER, and A. J. HEEGER, Solitons in polyacetylene, *Phys. Rev. Lett.* 42:1698 (1979).
3. D. N. CHRISTODOULIDES and R. I. JOSEPH, Discrete self-focusing in nonlinear arrays of coupled waveguides, *Opt. Lett.* 13:794–796 (1988).

4. P. BINDER, D. ABRAIMOV, A. V. USTINOV, S. FLACH, and Y. ZOLOTARYUK, Observation of breathers in Josephson ladders, *Phys. Rev. Lett.* 84:745 (2000).
5. A. TROMBETTONI and A. SMERZI, Discrete solitons and breathers with dilute Bose–Einstein condensates, *Phys. Rev. Lett.* 86:2353 (2001).
6. N. W. ASCHROFT and N. D. MERMIN, *Solid State Physics*, Saunders, Philadelphia, PA, 1976.
7. J. D. JOANNOPOULOS, R. D. MEADE, and J. D. WINN, *Photonic Crystals: Molding the Flow of Light*, Princeton University Press, Princeton, NJ, 1995.
8. Yu. KIVSHAR, Self-localization in arrays of de-focusing waveguides, *Opt. Lett.* 18:1147–1149 (1993).
9. Yu. KIVSHAR, W. KROLIKOWSKI, and O. A. CHUBYKALO, Dark solitons in discrete lattices, *Phys. Rev. E* 50:5020 (1994).
10. A. B. ACEVES, D. DE ANGELIS, T. PESCHEL, R. MUSCHALL, F. LEDERER, S. TRILLO, and S. WABNITZ, Discrete self-trapping, soliton interactions, and beam steering in nonlinear waveguide arrays, *Phys. Rev. E* 53:1172–1189 (1996).
11. S. AUBRY, Breathers in nonlinear lattices: Existence, linear stability and quantization, *Physica D* 103:201–250 (1997).
12. H. S. EISENBERG, Y. SILBERBERG, R. MORANDOTTI, A. R. BOYD, and J. S. AITCHISON, Discrete spatial optical solitons in waveguide arrays, *Phys. Rev. Lett.* 81:3383–3386 (1998).
13. S. DARMANYAN, S. KOPYAKOV, E. SCHMIDT, and F. LEDERER, Strongly localized vectorial modes in nonlinear waveguide arrays, *Phys. Rev. E* 57:3520–3530 (1988).
14. T. PESCHEL, U. PESCHEL, and F. LEDERER, Discrete bright solitary waves in quadratically nonlinear media, *Phys. Rev. E* 57:1127–1133 (1998).
15. R. MORANDOTTI, U. PESCHEL, J. S. AITCHISON, H. S. EISENBERG, and Y. SILBERBERG, Experimental observation of linear and nonlinear optical Bloch oscillations, *Phys. Rev. Lett.* 83:4755–4759 (1999).
16. T. PERTSCH, P. DANNBERG, W. ELFLEIN, A. BRAUER, and F. LEDERER, Optical Bloch oscillations in temperature tuned waveguide arrays, *Phys. Rev. Lett.* 83:4752–4755 (1999).
17. Z. G. CHEN, M. SEGEV, D. N. CHRISTODOULIDES, R. S. FEIGELSON, Waveguides formed by incoherent dark solitons, *Opt. Lett.* 24:1160–1162 (1999).
18. M. I. WEINSTEIN, Excitation thresholds for nonlinear localized modes on lattices, *Nonlinearity* 12:673–691 (1999).
19. H. S. EISENBERG, Y. SILBERBERG, R. MORANDOTTI, and J. S. AITCHISON, Diffraction management, *Phys. Rev. Lett.* 85:1863–1866 (2000).
20. B. MALOMED and P. G. KEVREKIDIS, Discrete vortex solitons, *Phys. Rev. E* 64:26601 (2001).
21. A. A. SUKHORUKOV and Y. S. KIVSHAR, Nonlinear localized waves in a periodic medium, *Phys. Rev. Lett.* 87:083901 (2001).
22. M. J. ABLOWITZ and Z. H. MUSSLIMANI, Discrete diffraction managed spatial solitons, *Phys. Rev. Lett.* 87:254102 (2001).
23. T. PERTSCH, T. ZENTGRAF, U. PESCHEL, A. BRAUER, and F. LEDERER, Anomalous refraction and diffraction in discrete optical systems, *Phys. Rev. Lett.* 88:093901 (2002).
24. N. K. EFREMIDIS, S. SEARS, D. N. CHRISTODOULIDES, J. W. FLEISCHER, and M. SEGEV, Discrete solitons in photorefractive optically induced photonic lattices, *Phys. Rev. E* 66:046602 (2002).
25. M. J. ABLOWITZ and Z. H. MUSSLIMANI, Discrete vector spatial solitons in a nonlinear waveguide array, *Phys. Rev. E* 65:056618 (2001).

26. J. W. FLEISCHER, T. CARMON, M. SEGEV, N. K. EFREMIDIS, and D. N. CHRISTODOULIDES, Observation of discrete solitons in optically-induced real time waveguide arrays, *Phys. Rev. Lett.* 90:023902 (2003).
27. J. W. FLEISCHER, M. SEGEV, N. K. EFREMIDIS, and D. N. CHRISTODOULIDES, Observation of two-dimensional discrete solitons in optically-induced nonlinear photonic lattices, *Nature (London)* 422:147 (2003).
28. D. MANDELIK, H. S. EISENBERG, Y. SILBERBERG, R. MORANDOTTI, and J. S. AITCHISON, Band-gap structure of waveguide arrays and excitation of Floquet-Bloch solitons, *Phys. Rev. Lett.* 90:053902 (2003).
29. D. N. CHRISTODOULIDES, F. LEDERER, and Y. SILBERBERG, Discretizing light behaviour in linear and nonlinear waveguide lattices, *Nature (London)* 424:817–823 (2003).
30. O. COHEN, T. SCHWARTZ, J. W. FLEISCHER, M. SEGEV, and D. N. CHRISTODOULIDES, Multiband vector lattice solitons, *Phys. Rev. Lett.* 91:113901 (2003).
31. A. A. SUKHORUKOV and Y. S. KIVSHAR, Multigap discrete vector solitons, *Phys. Rev. Lett.* 91:113902 (2003).
32. N. K. EFREMIDIS, J. HUDOCK, D. N. CHRISTODOULIDES, J. W. FLEISCHER, O. COHEN, and M. SEGEV, Two-dimensional optical lattice solitons, *Phys. Rev. Lett.* 91:213906 (2003).
33. A. A. SUKHORUKOV, D. NESHEV, W. KROLIKOWSKI, and Y. S. KIVSHAR, Nonlinear Bloch-wave interaction and bragg scattering in optically induced lattices, *Phys. Rev. Lett.* 92:093901 (2004).
34. J. W. FLEISCHER, G. BARTAL, O. COHEN, O. MANELA, M. SEGEV, J. HUDOCK, and D. N. CHRISTODOULIDES, Observation of vortex-ring discrete solitons in 2D photonic lattices, *Phys. Rev. Lett.* 92:123904 (2004).
35. D. N. NESHEV, T. J. ALEXANDER, E. A. OSTROVSKAYA, Y. S. KIVSHAR, H. MARTIN, I. MAKASYUK, and Z. CHEN, Observation of discrete vortex solitons in optically induced photonic lattices, *Phys. Rev. Lett.* 92:123903 (2004).
36. J. MEIER, G. I. STEGEMAN, D. N. CHRISTODOULIDES, Y. SILBERBERG, R. MORANDOTTI, H. YANG, G. SALAMO, M. SOREL, and J. S. AITCHISON, Experimental observation of discrete modulational instability, *Phys. Rev. Lett.* 92:163902 (2004).
37. H. BULJAN, O. COHEN, J. W. FLEISCHER, T. SCHWARTZ, M. SEGEV, Z. H. MUSSLIMANI, N. K. EFREMIDIS, and D. N. CHRISTODOULIDES, Random-phase solitons in nonlinear periodic lattices, *Phys. Rev. Lett.* 92:223901 (2004).
38. A. FRATALOCCHI, G. ASSANTO, K. A. BRZDAKIEWICZ, and M. A. KARPIERZ, Discrete propagation and spatial solitons in nematic liquid crystals, *Opt. Lett.* 29:1530–1532 (2004).
39. O. MANELA, O. COHEN, G. BARTAL, J. W. FLEISCHER, and M. SEGEV, Two-dimensional higher-band vortex lattice solitons, *Opt. Lett.* 29:2049–2051 (2004).
40. U. PESCHEL, O. EGOROV, and F. LEDERER, Discrete cavity soliton, *Opt. Lett.* 29:1909–1911 (2004).
41. J. K. YANG, I. MAKASYUK, A. BEZRYADINA, and Z. CHEN, Dipole solitons in optically induced two-dimensional photonic lattices, *Opt. Lett.* 29:1662–1664 (2004).
42. Z. G. CHEN, A. BEZRYADINA, I. MAKASYUK, and J. K. YANG, Observation of two-dimensional lattice vector solitons, *Opt. Lett.* 29:1656–1658 (2004).
43. H. MARTIN, E. D. EUGENIEVA, Z. CHEN, and D. N. CHRISTODOULIDES, Discrete solitons and soliton induced dislocations in partially coherent photonic lattices, *Phys. Rev. Lett.* 92:123902 (2004).
44. R. IWANOV, R. SCHIEK, G. I. STEGEMAN, T. PERTSCH, F. LEDERER, Y. MIN, and W. SOHLER, Observation of discrete quadratic solitons, *Phys. Rev. Lett.* 93:113902 (2004).

45. O. COHEN, G. BARTAL, H. BULJAN, J. W. FLEISCHER, T. CARMON, M. SEGEV, and D. N. CHRISTODOULIDES, Observation of random-phase lattice solitons, *Nature (London)* 433:500 (2005).
46. G. BARTAL, O. COHEN, H. BULJAN, J. W. FLEISCHER, O. MANELA, M. SEGER, Brillouin zone spectroscopy of linear and nonlinear photonic lattices, *Phys. Rev. Lett.* 94:163902 (2005).
47. M. SOLJAČIĆ and J. D. JOANOPOLUOS, Enhancement of nonlinear effects using photonic crystals, *Nat. Mater.* 3:211–219 (2004).
48. Y. S. KIVSHAR and S. FLACH, Eds., Focus issue—Nonlinear localized modes: Physics and applications, *Chaos* 13:586–799 (2003).
49. D. CAMPBELL, S. FLACH, and Y. S. KIVSHAR, Localizing energy through nonlinearity and discreteness, *Phys. Today* 57:43–49 (2004).
50. M. MITCHELL, Z. CHEN, M. SHIH, and M. SEGEV, Self-trapping of partially spatially incoherent light, *Phys. Rev. Lett.* 77:490–493 (1996).
51. M. MITCHELL and M. SEGEV, Self-trapping of incoherent white light, *Nature (London)* 387:880–882 (1997).
52. D. N. CHRISTODOULIDES, T. H. COSKUN, M. MITCHELL, and M. SEGEV, Theory of incoherent self-focusing in biased photorefractive media, *Phys. Rev. Lett.* 78:646–649 (1997).
53. M. MITCHELL, M. SEGEV, T. H. COSKUN, and D. N. CHRISTODOULIDES, Theory of self-trapped spatially incoherent light beams, *Phys. Rev. Lett.* 79:4990–4993 (1997).
54. Z. G. CHEN, M. MITCHELL, M. SEGEV, T. H. COSKUN, and D. N. CHRISTODOULIDES, Self-trapping of dark incoherent light beams, *Science* 280:889–892 (1998).
55. A. W. SNYDER and D. J. MITCHELL, Big incoherent solitons, *Phys. Rev. Lett.* 80:1422–1425 (1998).
56. D. N. CHRISTODOULIDES, T. H. COSKUN, M. MITCHELL, Z. CHEN, and M. SEGEV, Theory of incoherent dark solitons, *Phys. Rev. Lett.* 80:5113–5116 (1998).
57. V. V. SHKUNOV and D. ANDERSON, Radiation transfer model of self-trapping spatially incoherent radiation by nonlinear media, *Phys. Rev. Lett.* 81:2683–2686 (1998).
58. N. AKHMEDIEV, W. KROLIKOWSKI, and A. W. SNYDER, Partially coherent solitons of variable shape, *Phys. Rev. Lett.* 81:4632–4635 (1998).
59. O. BANG, D. EDMUNDSON, and W. KROLIKOWSKI, Collapse of incoherent light beams in inertial bulk Kerr media, *Phys. Rev. Lett.* 83:5479–5482 (1999).
60. M. SOLJAČIĆ, M. SEGEV, T. H. COSKUN, D. N. CHRISTODOULIDES, and A. VISHWANATH, Modulation instability of incoherent beams in noninstantaneous nonlinear media, *Phys. Rev. Lett.* 84:467–470 (2000).
61. T. COSKUN, D. N. CHRISTODOULIDES, Y. KIM, Z. CHEN, M. SOLJAČIĆ, and M. SEGEV, Bright spatial solitons on a partially incoherent background, *Phys. Rev. Lett.* 84:2374 (2000).
62. D. KIP, M. SOLJAČIĆ, M. SEGEV, E. EUGENIEVA, and D. N. CHRISTODOULIDES, Modulation instability and pattern formation in spatially incoherent light beams, *Science* 290:495–498 (2000).
63. C. ANASTASSIOU, M. SOLJAČIĆ, M. SEGEV, D. KIP, E. EUGENIEVA, D. N. CHRISTODOULIDES, and Z. H. MUSSLIMANI, Eliminating the transverse instabilities of Kerr solitons, *Phys. Rev. Lett.* 85:4888–4891 (2000).
64. D. N. CHRISTODOULIDES, E. D. EUGENIEVA, T. H. COSKUN, M. SEGEV, and M. MITCHELL, Equivalence of three approaches describing incoherent wave propagation in inertial nonlinear media, *Phys. Rev. E* 63:035601 (2001).
65. J. KLINGER, H. MARTIN, and Z. CHEN, Experiments on induced modulational instability of an incoherent optical beam, *Opt. Lett.* 26:271–273 (2001).

66. M. PECCIANI and G. ASSANTO, Incoherent spatial solitary waves in nematic liquid crystals, *Opt. Lett.* 26:1791–1793 (2001).
67. M. SEGEV and D. N. CHRISTODOULIDES, *Incoherent Solitons in Spatial Solitons* (S. TRILLO and W. TORRUELLAS, Eds.), pp. 87–125, Springer, Berlin, 2001.
68. Z. CHEN, S. M. SEARS, H. MARTIN, D. N. CHRISTODOULIDES and M. SEGEV, Clustering of solitons in weakly correlated wavefronts, *Proc. Natl. Acad. Sci. USA* 99:5223–5227 (2002).
69. B. HALL, M. LISAK, D. ANDERSON, R. FEDELE, and V. E. SEMENOV, Statistical theory for incoherent light propagation in nonlinear media, *Phys. Rev. E* 65:035602 (2002).
70. H. BULJAN, A. ŠIBER, M. SOLJAČIĆ, and M. SEGEV, Propagation of incoherent white light and modulation instability in noninstantaneous nonlinear media, *Phys. Rev. E* 66:035601 (2002).
71. H. BULJAN, M. SEGEV, M. SOLJAČIĆ, N. K. EFREMIDIS, and D. N. CHRISTODOULIDES, White-light solitons, *Opt. Lett.* 28:1239–1241 (2003).
72. O. KATZ, T. CARMON, T. SCHWARTZ, M. SEGEV, and D. N. CHRISTODOULIDES, Observation of elliptic incoherent spatial solitons, *Opt. Lett.* 29:1248–1250 (2004).
73. C. C. JENG, M. F. SHIH, K. MOTZEK, and Y. S. KIVSHAR, Partially incoherent optical vortices in self-focusing nonlinear media, *Phys. Rev. Lett.* 92:043904 (2004).
74. A. PICOZZI, M. HAELTERMAN, S. PITOIS, and G. MILLOT, Incoherent solitons in instantaneous response nonlinear media, *Phys. Rev. Lett.* 92:143906 (2004).
75. W. KROLIKOWSKI, O. BANG, J. WYLLER, Nonlocal incoherent solitons, *Phys. Rev. E* 70:036617 (2004).
76. T. SCHWARTZ, T. CARMON, H. BULJAN, and M. SEGEV, Spontaneous pattern formation with incoherent white light, *Phys. Rev. Lett.* 93: (2004).
77. O. COHEN, H. BULJAN, T. SCHWARTZ, J. W. FLEISCHER, and M. SEGEV, Random-phase spatial solitons in instantaneous nonlocal nonlinear media, arXiv nlin.PS/0410031 (2004).
78. L. MANDEL and E. WOLF, *Optical Coherence and Quantum Optics*, Cambridge University Press, New York, 1995.
79. J. GOODMAN, *Statistical Optics*, John Wiley & Sons, New York, 1985.
80. E. FERMI, J. PASTA, and S. ULAM, Los Alamos Rpt. LA-1940 (1955).

UNIVERSITY OF ZAGREB
ISRAEL INSTITUTE OF TECHNOLOGY
PRINCETON UNIVERSITY
UNIVERSITY OF CENTRAL FLORIDA

(Received January 14, 2005)